

**How the forest interacts with the trees:  
Multiscale shape integration explains global and local processing**

Georgin Jacob<sup>1,2</sup> and S. P. Arun<sup>1\*</sup>

<sup>1</sup>Centre for Neuroscience & <sup>2</sup>Department of Electrical Communication Engineering

Indian Institute of Science, Bangalore-560012

\*Correspondence to [sparun@iisc.ac.in](mailto:sparun@iisc.ac.in)

Abbreviated Title : Global processing explained by shape integration

Number of Figures : 11

1

## ABSTRACT

2        Hierarchical stimuli (such as a circle made of diamonds) have been widely used to  
3        study global and local processing. Two classic phenomena have been observed using  
4        these stimuli: the global advantage effect (that we identify the circle faster than the  
5        diamonds) and the incongruence effect (that we identify the circle faster when both global  
6        and local shapes are circles). Understanding them has been difficult because they occur  
7        during shape detection, where an unknown categorical judgement is made on an  
8        unknown feature representation.

9        Here we report two essential findings. First, these phenomena are present both in  
10       a general same-different task and a visual search task, suggesting that they may be  
11       intrinsic properties of the underlying representation. Second, in both tasks, responses  
12       were explained using linear models that combined multiscale shape differences and  
13       shape distinctiveness. Thus, global and local processing can be understood as properties  
14       of a systematic underlying feature representation.

15

## INTRODUCTION

16 Visual objects contain features at multiple spatial scales (Oliva and Schyns, 1997;  
17 Morrison and Schyns, 2001; Ullman et al., 2002). Our perception of global and local shape  
18 have been extensively investigated using hierarchical stimuli, which contain local  
19 elements arranged to form a global shape (Figure 1). Two classic phenomena have been  
20 observed using these stimuli (Navon, 1977; Kimchi, 1992). First, the global shape can be  
21 detected faster than the local shape; this is known as the global advantage effect. Second,  
22 the global shape can be detected faster in a congruent shape (e.g. circle made of circles)  
23 than in an incongruent shape (e.g. circle made of diamonds); this is known as the global-  
24 local incongruence effect. Subsequent studies have shown that these effects depend on  
25 the size, position, spacing and arrangement of the local shapes (Lamb and Robertson,  
26 1990; Kimchi, 1992; Malinowski et al., 2002; Miller and Navon, 2002).

27 These global/local processing phenomena have since been extensively  
28 investigated for their neural basis as well as their application to a variety of disorders.  
29 Global and local processing are thought to be localized to the right and left hemispheres  
30 respectively (Fink et al., 1996; Han et al., 2002, 2004), and are mediated by brain  
31 oscillations at different frequencies (Romei et al., 2011; Liu and Luo, 2019). These  
32 phenomena have now been observed in a variety of other animals, especially during tasks  
33 that require speeded responses (Tanaka and Fujita, 2000; Cavoto and Cook, 2001; Pitteri  
34 et al., 2014; Avarguès-Weber et al., 2015). Global/local processing is impaired in a variety  
35 of clinical disorders (Bihrlle et al., 1989; Robertson and Lamb, 1991; Slavin et al., 2002;  
36 Behrmann et al., 2006; Song and Hakoda, 2015), including those related to reading  
37 (Lachmann and Van Leeuwen, 2008; Franceschini et al., 2017). Finally, individual  
38 differences in global/local processing predict other aspects of object perception (Gerlach  
39 and Poirel, 2018; Gerlach and Starrfelt, 2018).

40           Despite these insights, we lack a deeper understanding of these phenomena for  
41   several reasons. First, they have only been observed during shape detection tasks, which  
42   involve two complex steps: a categorical response made over a complex underlying  
43   representation (Freedman and Miller, 2008; Mohan and Arun, 2012). It is therefore  
44   possible that these phenomena reflect the priorities of the categorical decision.  
45   Alternatively, they may reflect some intrinsic property of the underlying shape  
46   representation.

47           Second, these shape detection tasks, by their design, set up a response conflict  
48   for incongruent but not congruent stimuli. This is because the incongruent stimulus  
49   contains two different shapes at the global and local levels, each associated with a  
50   different response during the global and local blocks. By contrast there is no such conflict  
51   for congruent stimuli where the global and local shapes are identical. Thus, the  
52   incongruence effect might reflect the response conflicts associated with making opposite  
53   responses in the global and local blocks (Miller and Navon, 2002). Alternatively, again, it  
54   might reflect some intrinsic property of the underlying shape representation.

55           Third, it has long been appreciated that these phenomena depend on stimulus  
56   properties such as the size, position, spacing and arrangement of the local elements  
57   (Lamb and Robertson, 1990; Kimchi, 1992; Malinowski et al., 2002; Miller and Navon,  
58   2002). Surprisingly, hierarchical stimuli themselves have never been studied from the  
59   perspective of feature integration i.e. how the global and local shapes combine. A deeper  
60   understanding of how hierarchical stimuli are organized in perception can elucidate how  
61   these stimulus properties affect global/local processing.

62           Thus, understanding the global advantage and incongruence effects will require  
63   reproducing them in simpler tasks, as well as understanding how global and local shape  
64   combine in the perception of hierarchical stimuli. This is not only a fundamental question

65 but has clinical significance since deficits in global/local processing have been reported  
66 in a variety of disorders.

67

## 68 **Overview of this study**

69 Here we addressed the above limitations as follows. First, we devised a simpler  
70 shape task which involves subjects indicating whether two shapes are the same or  
71 different at either the global or local level. This avoids any effects due to specific shapes  
72 but still involves categorization, albeit a more general one. Second, we devised a visual  
73 search task in which subjects had to report the location of an oddball target. This task  
74 avoids any categorical judgement and the accompanying response conflicts. It also does  
75 not involve any explicit manipulation of global vs local attention unlike the global/local  
76 processing tasks. If these phenomena are present in visual search, it would imply that  
77 they reflect properties of the underlying shape representation of hierarchical stimuli. If not,  
78 they must arise from the categorization process.

79 To understand how global and local shape combine in visual search, we asked  
80 how search difficulty for a target differing in both global and local shape from the  
81 distractors can be understood in terms of global and local shape differences. While search  
82 reaction time (RT) is the natural observation made during any search task, we have  
83 shown recently that its reciprocal (1/RT) is the more useful measure for understanding  
84 visual search (Arun, 2012; Pramod and Arun, 2014). The reciprocal of search time can  
85 be thought of as the dissimilarity between the target and distractors in visual search, and  
86 has the intuitive interpretation as the underlying salience signal that accumulates to  
87 threshold (Arun, 2012). Models based on 1/RT consistently outperform models based  
88 directly on search time (Vighneshvel and Arun, 2013; Pramod and Arun, 2014, 2016;

89 Sunder and Arun, 2016). Further, using this measure, a variety of object attributes as well  
90 as top-down factors such as target preview have been found to combine linearly.

91 We performed two experiments. In Experiment 1, we replicated the global  
92 advantage and incongruence effects in a generic same-different task. We then show that  
93 image-by-image variations in response times can be explained by two factors:  
94 dissimilarity and distinctiveness. In Experiment 2, we show that these effects can be  
95 observed even when subjects perform visual search on the same stimuli. We also show  
96 that visual search for hierarchical stimuli can be accurately explained as a linear sum of  
97 global and local feature relations. Finally we show that the factors driving the same-  
98 different task responses are closely related to the visual search model.

99

## EXPERIMENT 1: SAME-DIFFERENT TASK

100 In most studies of global and local processing, subjects are required to indicate  
101 which of two target shapes they saw at the global or local levels (Navon, 1977; Kimchi,  
102 1994). This approach severely limits the number of shapes that can be tested because of  
103 the combinatorial increase in the number of possible shape pairs. To overcome this  
104 limitation, we devised a same-different task in which subjects have to indicate whether  
105 two simultaneously presented shapes contain the same or different shape at the global  
106 or local level. Of particular interest to us were two questions: (1) Are the global advantage  
107 and incongruence effects observable in this more general shape detection task? (2) Do  
108 response times in this task systematically vary across stimuli and across the global and  
109 local blocks?

110

111

## METHODS

112 Here and in all experiments, subjects had normal or corrected-to-normal vision and  
113 gave written informed consent to an experimental protocol approved by the Institutional  
114 Human Ethics Committee of the Indian Institute of Science, Bangalore. Subjects were  
115 naive to the purpose of the experiment and received monetary compensation for their  
116 participation.

117

118 *Subjects.* Sixteen human subjects (11 male, aged 20-30 years) participated in this  
119 experiment. We chose this number of subjects based on previous studies of object  
120 categorization from our lab in which this sample size yielded consistent responses  
121 (Mohan and Arun, 2012).

122

123 *Stimuli.* We created hierarchical stimuli by placing eight local shapes uniformly along the  
124 perimeter of a global shape. All local shapes had the same area (0.77 squared degrees  
125 of visual angle), and all global shapes occupied an area that was 25 times larger. We  
126 used seven distinct shapes at the global and local levels to create 49 hierarchical stimuli  
127 (all stimuli can be seen in Figure 8). Stimuli were shown as white against a black  
128 background.

129  
130 *Procedure.* Subjects were seated ~60 cm from a computer monitor under the control of  
131 custom programs written in MATLAB with routines from PsychToolbox (Brainard, 1997).  
132 Subjects performed two blocks of the same-different task, corresponding to global or local  
133 shape matching. In both blocks, a pair of hierarchical shapes were shown to the subject  
134 and the subject had to respond if the shapes contained the same or different shape at a  
135 particular global/local level (key “Z” for same, “M” for different). Each block started with a  
136 practice block with eight trials involving hierarchical stimuli made of shapes that were not  
137 used in the main experiment. Subjects were given feedback after each trial during the  
138 practice block.

139 In all blocks, each trial started with a red fixation cross (measuring 0.6° by 0.6°)  
140 presented at the centre of the screen for 750 ms. This was followed by two hierarchical  
141 stimuli (with local elements measuring 0.6° along the longer dimension and longest  
142 dimension of global shapes are 3.8°) presented on either side of the fixation cross,  
143 separated by 8° from center to center. The position of each stimulus was jittered by  $\pm 0.8^\circ$   
144 uniformly at random along the horizontal and vertical. These two stimuli were shown for  
145 200 ms followed by a blank screen until the subject made a response, or until 5 seconds,  
146 whichever was sooner.

147

148 *Stimulus pairs.* To avoid any response bias, we selected stimulus pairs in each block such  
149 that the proportion of same- and different-responses were equal. Each block consisted of  
150 588 stimulus pairs. These pairs were divided equally into four groups of 147 pairs (Figure  
151 1A): (1) Pairs with global shape same, local shape same (GSLS, i.e. identical shapes);  
152 (2) Pairs with global shape same but local different (GSLD); (3) Pairs with global different  
153 but local same (GDLS) and (4) Pairs with both global and local shape different (GDLD).  
154 Since there were different number of total possible pairs in each category we selected  
155 pairs as follows: for GSLS pairs, there are 49 unique stimuli and therefore 49 pairs, so we  
156 repeated each pair three times to obtain 147 pairs. For GSLD and GDLS pairs, there are  
157 147 unique pairs, so each pair was used exactly once. For GDLD pairs, there are 441  
158 possible pairs, so we selected 147 pairs which consisted of 21 congruent pairs (i.e. each  
159 stimulus containing identical global and local shapes), 21 incongruent pairs (in which  
160 global shape of one stimulus was the local shape of the other, and vice-versa), and 105  
161 randomly chosen other pairs. The full set of 588 stimulus pairs were fixed across all  
162 subjects. Each stimulus pair was shown twice. Thus each block consisted of  $588 \times 2 =$   
163 1176 trials. Error trials were repeated after a random number of other trials.

164 We removed inordinately long or short response times for each image pair using  
165 an automatic outlier detection procedure (*isoutlier* function, MATLAB 2018). We pooled  
166 the reaction times across subjects for each image pair, and all response times greater  
167 than three scaled median absolute deviations away from the median were removed. In  
168 practice this procedure removed ~8% of the total responses.

169

170 *Estimating data reliability.*

171 To estimate an upper limit on the performance of any model, we reasoned that the  
172 performance of any model cannot exceed the reliability of the data itself. To estimate the

173 reliability of the data, we first calculated the average correlation between two halves of  
174 the data. However, doing so underestimates the true reliability since the correlation is  
175 based on two halves of the data rather than the entire dataset. To estimate this true  
176 reliability we applied a Spearman-Brown correction on the split-half correlation. This  
177 Spearman-Brown corrected correlation ( $rc$ ) is given by  $rc = 2r/(1+r)$  where  $r$  is the  
178 correlation between the two halves. This data reliability is denoted as  $rc$  throughout the  
179 text to distinguish it from the standard Pearson's correlation coefficient (denoted as  $r$ ).

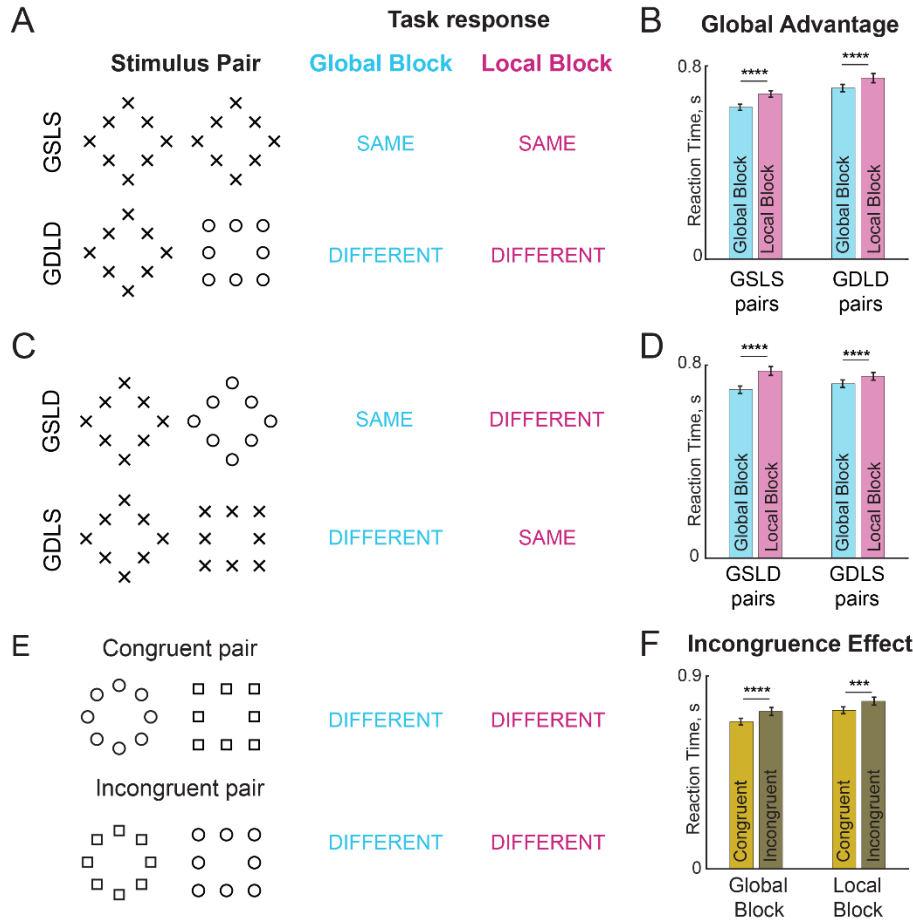
180

## RESULTS

181        Here, subject performed a same-different task in which they reported whether a  
182        pair of hierarchical stimuli contained the same/different shape at the global level or at the  
183        local level in separate blocks. We grouped the image pairs into four distinct types based  
184        on whether the shapes were same/different at the global/local levels. The first type  
185        comprised pairs with no difference at the global or local levels, i.e. identical images,  
186        denoted by GSLS (Figure 1A, top row). The second type comprised pairs in which both  
187        global and local shape were different, denoted by GDLD (Figure 1A, bottom row). These  
188        two were pairs elicited identical responses in the global and local blocks. The third type  
189        comprised pairs with the same global shape but different local shapes, denoted by GSLD  
190        (Figure 1C, top row). The fourth type comprised pairs differing in global shape but with  
191        identical local shapes, denoted by GDLS (Figure 1C, bottom row). These two were pairs  
192        that elicited opposite responses in the global and local blocks. Since both blocks  
193        consisted of identical image pairs, the responses in the two blocks are directly  
194        comparable and matched for image content.

195

196



197  
198 **Figure 1. Same-different task for global-local processing.** In the global block, subjects  
199 have to indicate whether a pair of images presented contain the same shape at the global  
200 level. Likewise in the local block, they have to make same-different judgments about the  
201 shape at the local level. Block order was counterbalanced across subjects.  
202 (A) Example image-pairs with identical correct responses in the global and local blocks.  
203 In the GSLS pairs, both images are identical i.e. have the same global shape and  
204 same local shape. In the GDLD pairs, the two images differ in both global shape and  
205 local shape.  
206 (B) Bar plot comparing average response times for GSLS and GDLD pairs. Error bars  
207 indicate s.e.m. across subjects. Asterisks indicate statistical significance assessed  
208 using an ANOVA on response times (\*\*\*\* is  $p < 0.00005$ ).  
209 (C) Example image pairs that elicited opposite responses in the global and local blocks.  
210 In the GSLD pairs, the two images contain the same global shape but differ in local  
211 shape – thus the correct response is “SAME” in the global block but “DIFFERENT” in  
212 the local block. In the GDLS pairs, the two images contain the same local shape but  
213 differ in global shape, resulting again in opposite responses in the two blocks.  
214 (D) Same as B but for GSLD and GDLS pairs.  
215 (E) Example congruent and incongruent image pairs. Congruent image pairs comprised  
216 stimuli with the same shape at the global and local levels. In the incongruent image  
217 pairs, the global shape of one image matched the local shape of the other, and vice-  
218 versa. Thus each congruent image pair was exactly matched to an incongruent image  
219 pair.  
220 (F) Bar plot of average response times for congruent and incongruent image pairs.  
221 Asterisks indicate statistical significance using an ANOVA on response times (\*\*\*\* is  
222  $p < 0.00005$ ).

223 **Is there a global advantage in the same-different task?**

224 Subjects were highly accurate in the task overall, but were more accurate in the  
225 global block (mean & std of accuracy across subjects:  $91\% \pm 4\%$  in the global block;  
226  $88\% \pm 7\%$  in the local block,  $p < 0.05$ , sign-rank test on subject-wise accuracy in the two  
227 blocks). They were also significantly faster in the global block (mean & std of response  
228 times across subjects:  $702 \pm 55.7$  ms in the global block;  $752 \pm 66.7$  ms in the local block;  
229  $p < 0.005$ , sign-rank test on subject-wise average RTs in the two blocks). This pattern  
230 was true both for image pairs that elicited identical responses in the two blocks (GSLS &  
231 GDLD pairs; Figure 1B) as well as for those that elicited opposite responses (GDLS &  
232 GSLD pairs; Figure 1C). Thus, subjects were faster and more accurate in the global block  
233 across all image pairs, reflecting a robust global advantage.

234

235 **Is there an incongruence effect in the same-different task?**

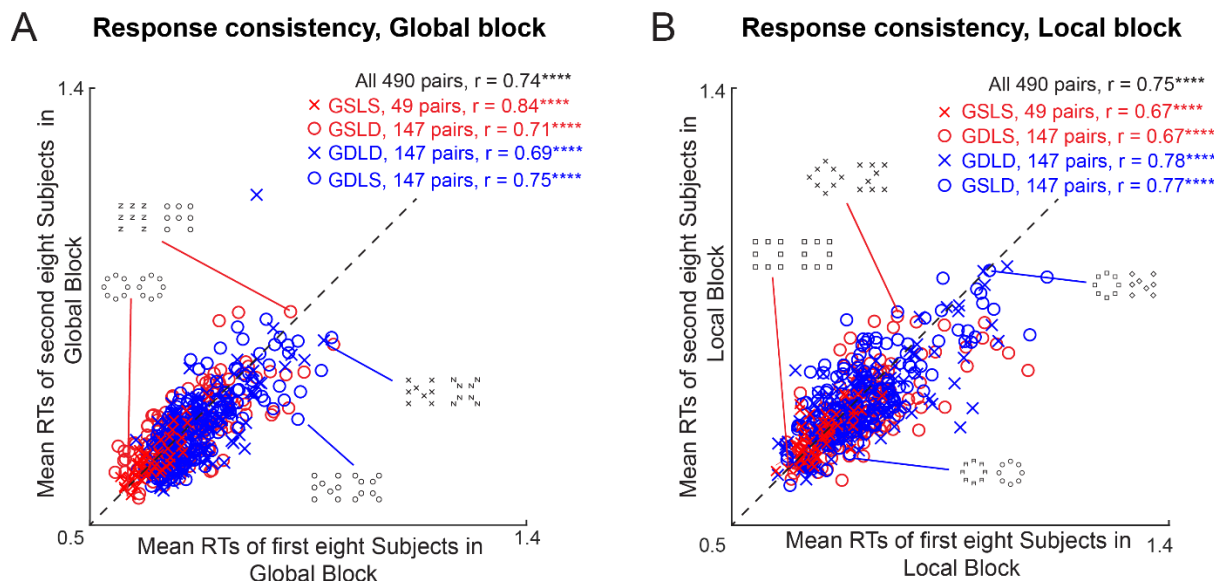
236 Next we asked whether the incongruence effect can be observed in the same-  
237 different task. To this end we compared the average RT for GDLD image pairs in which  
238 the two images were either both congruent or both incongruent (Figure 1E). Subjects  
239 responded significantly faster to congruent compared to incongruent pairs (Figure 1F).  
240 To assess the statistical significance of these effects, we performed an ANOVA on the  
241 response times with subject (16 levels), block (2 levels), congruence (2 levels) and image  
242 pair (21 levels) as factors. This revealed a significant main effect of congruence ( $p <$   
243  $0.00005$ ), but also main effects of subject and block ( $p < 0.00005$  in all cases), as well as  
244 significant interaction effects ( $p < 0.00005$ , between subjects and blocks; all other effects  
245 were  $p > 0.05$ ). We conclude that there is a robust incongruence effect in both the global  
246 and local blocks.

247

248 **Do responses in the same-different task vary systematically across image pairs?**

249 Having established that subjects show a global advantage and incongruence  
250 effects in the same-different task, we wondered whether there were any other systematic  
251 variations in response times across image pairs. Specifically, we asked whether image  
252 pairs that evoked fast responses in one group of subjects would also elicit a fast response  
253 in another group of subjects. This was indeed the case: we found a significant correlation  
254 between the average response times of the first and second half of all subjects in both  
255 the global block ( $r = 0.74$ ,  $p < 0.00005$ ; Figure 2A) and the local block ( $r = 0.75$ ,  $p <$   
256  $0.000005$ ; Figure 2B). This correlation was present in all four image types as well in both  
257 blocks (Figure 2).

258



259  
260 **Figure 2. Consistency of response times in the same-different task**  
261 (A) Average response times for one half of the subjects in the global block of the same-  
262 different task plotted against those of the other half. Asterisks indicate statistical  
263 significance (\* is  $p < 0.05$ , \*\* is  $p < 0.005$  etc).  
264 (B) Same as (A) but for the local block.

265  
266 **Are responses in the global and local block related?**

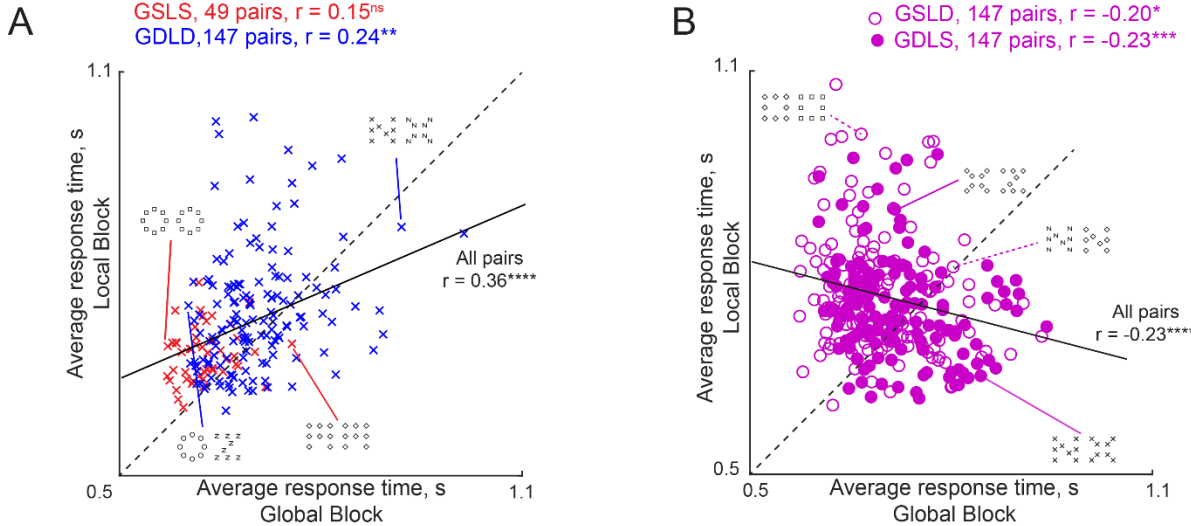
267 Having established that response times are systematic within each block, we next  
268 investigated how responses in the global and local block are related for the same image

269 pairs presented in both blocks. First, we compared responses to image pairs that elicit  
270 identical responses in both blocks. These are the GSLS pairs (which elicit a SAME  
271 response in both blocks) and GDLD pairs (that elicit a DIFFERENT response in both  
272 blocks). This revealed a positive but not significant correlation between the responses to  
273 the GSLS pairs in both blocks ( $r = 0.15$ ,  $p = 0.32$  across 49 image pairs; Figure 3A). By  
274 contrast the responses to the GDLD pairs, which were many more in number ( $n = 147$ ),  
275 showed a significant positive correlation between the global and local blocks ( $r = 0.24$ ,  $p$   
276  $< 0.005$ ; Figure 3A). Second, we compared image pairs that elicited opposite responses  
277 in the global and local blocks, namely the GSLD and GDLS pairs. This revealed a  
278 significant negative correlation in both cases ( $r = -0.20$ ,  $p < 0.05$  for GSLD pairs,  $r = -0.23$ ,  
279  $p < 0.0005$  for GDLS pairs; Figure 3B). Thus, image pairs that are hard to categorize as  
280 SAME are easier to categorize as DIFFERENT.

281 Note that in all cases, the correlation between responses in the global and local  
282 blocks were relatively small (only  $r = \sim 0.2$ ; Figure 3) compared to the consistency of the  
283 responses within each block (split-half correlation = 0.75 in the global block; 0.74 in the  
284 local block;  $p < 0.00005$  for both the conditions; Figure 2). These low correlations suggest  
285 that responses in the global and local blocks are qualitatively different.

286

287



288

289

**Figure 3. Responses to hierarchical stimuli in global and local blocks.**

290

291

292

293

294

295

296

297

298

299

(A) Average response times in the local block plotted against the global block, for image pairs with identical responses in the global and local blocks. These are the GSLS pairs (red crosses,  $n = 49$ ) which elicited the "SAME" response in both blocks, and the GDLD pairs (blue crosses,  $n = 147$ ) which elicited the "DIFFERENT" responses in both blocks.

(B) Average response times in the local block plotted against the global block, for image pairs with opposite responses in the global and local blocks. These are the GSDL pairs (open circles,  $n = 147$ ) which elicit the "SAME" response in the global block but the "DIFFERENT" response in the local block, and the GDLS pairs (filled circles,  $n = 147$ ) which likewise elicit opposite responses in the two blocks.

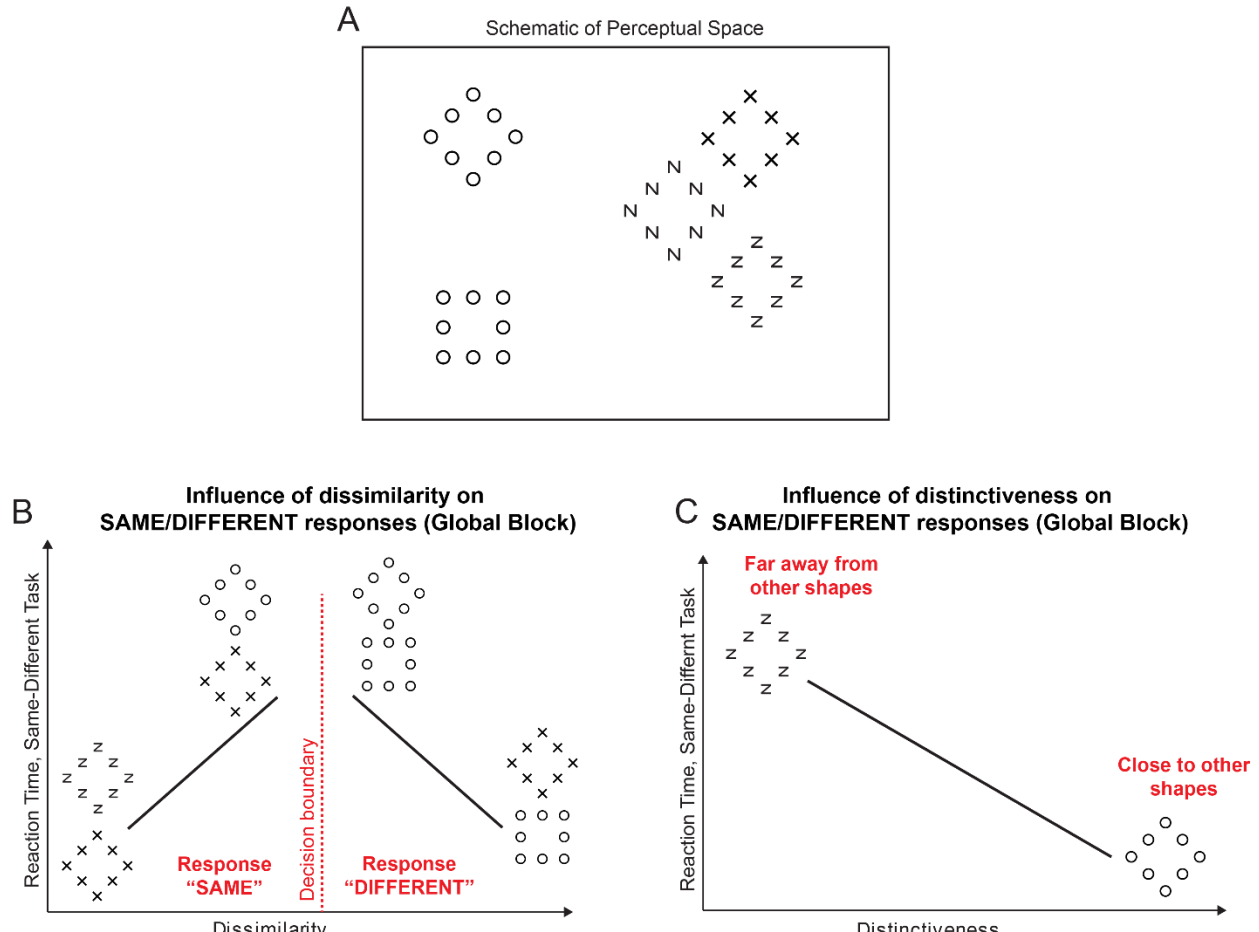
300

301 **What factors influence response times in the same-different task?**

302 So far we have shown that the global advantage and incongruence effects are  
303 present in a same-different task, and that response times vary systematically in each  
304 block across image pairs. However these findings do not explain why some image pairs  
305 elicit slower responses than others (Figure 2).

306 Consider a schematic of perceptual space depicted in Figure 4A. We hypothesized  
307 that the response time for an image pair in the global block could depend on two factors.  
308 The first factor is the dissimilarity between the two images. If the two images have the  
309 same global shape (thus requiring a “SAME” response), then the response time would be  
310 proportionally longer as the local shapes become more dissimilar. By contrast, if two  
311 images differ in global shape (thus requiring a “DIFFERENT” response), then the  
312 response time would be shorter if the two images are more dissimilar (Figure 4B). Thus,  
313 shape dissimilarity between the two images can have opposite effects on response time  
314 depending on whether the response is same or different. The second factor is the  
315 distinctiveness of the images relative to all other images. We reasoned that a shape that  
316 is distinct from all other shapes should evoke a faster response since there are fewer  
317 competing stimuli in its vicinity. This factor is required to explain systematic variation in  
318 response times for identical images (e.g. GSLS pairs) where the first factor (dissimilarity)  
319 plays no role. But more generally, distinctiveness could play a role even when both  
320 images are different. Below we describe how distinctiveness and dissimilarity can be used  
321 to predict response time variations in the same-different task.

322



325 (A) To elucidate how same-different responses are related to the underlying perceptual  
326 space, consider a perceptual space consisting of many hierarchical stimuli. In this  
327 space, nearby stimuli are perceptually similar.

328 (B) We hypothesized that subjects make “SAME” or “DIFFERENT” responses to an image  
329 pair driven by the dissimilarity between the two images. In the global block, when two  
330 images have the same global shape, we predict that response times are longer when  
331 the two images are more dissimilar. Thus, two diamonds made using Xs and Zs evoke  
332 a faster response than two diamonds made of circles or Xs, because the latter pair is  
333 more dissimilar than the former. By contrast, when two images differ in global shape,  
334 responses are faster when they are more dissimilar.

335 (C) We also hypothesized that shapes that are more distinct i.e. far away from other  
336 shapes will elicit faster responses because there are no surrounding distractors. Thus,  
337 the diamond made of circles, which is far away from all other stimuli in panel A, will  
338 elicit a faster response than a diamond made of Zs.

339

340 **Effect of distinctiveness on same-different responses in the global block**

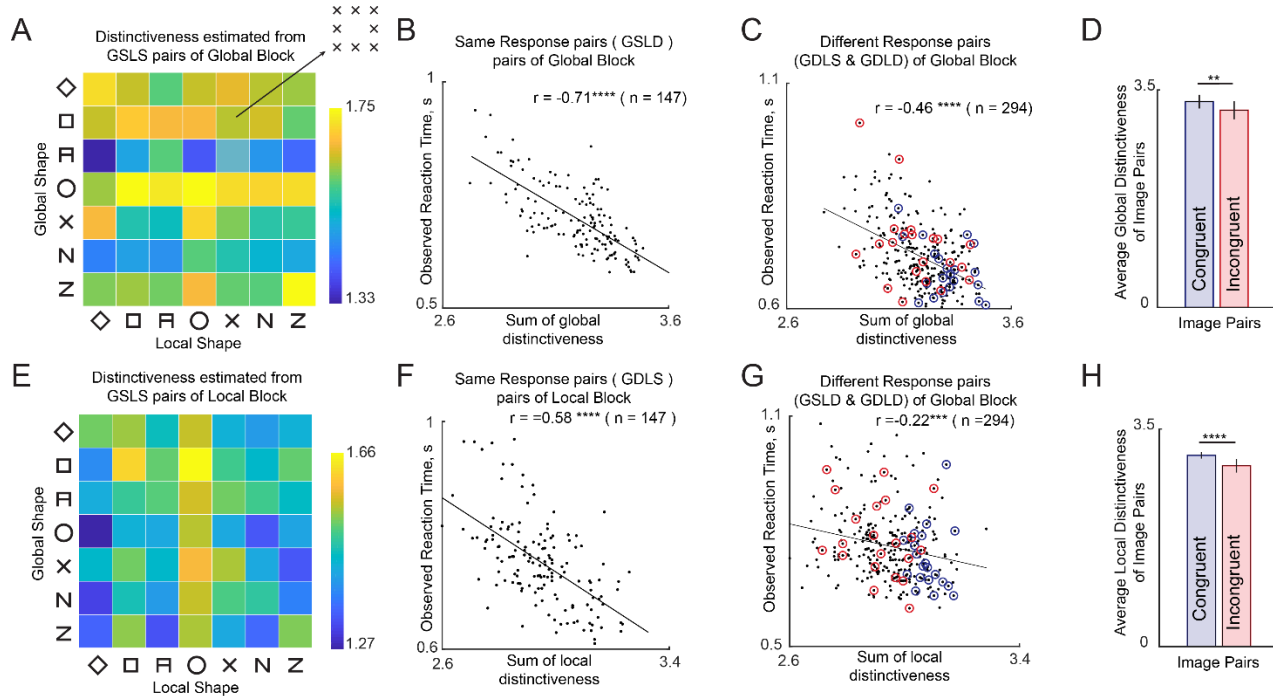
341 How do we estimate distinctiveness? We reasoned that if distinctiveness was the  
342 only influence on response time to identical images, then images that elicited fast  
343 responses must be more distinctive than those that elicit slow responses. We therefore  
344 took the reciprocal of the average response time for each GSLS pair (across trials and  
345 subjects) as a measure of distinctiveness for that image. The estimated distinctiveness  
346 for the hierarchical stimuli in the global block is depicted in Figure 5A. It can be seen that  
347 shapes with a global circle (“O”) are more distinctive than shapes containing the global  
348 shape “A”. In other words, subjects responded faster when they saw these shapes.

349 Having estimated distinctiveness of each image using the GSLS pairs, we asked  
350 whether it would predict responses to other pairs. For each image pair containing two  
351 different images, we calculated the net distinctiveness as the sum of the distinctiveness  
352 of the two individual images. We then plotted the average response times for each GSLS  
353 pair (which evoked a “SAME” response) in the global block against the net distinctiveness.  
354 This revealed a striking negative correlation ( $r = -0.71$ ,  $p < 0.00005$ ; Figure 5B). In other  
355 words, subjects responded quickly to distinctive images. We performed a similar analysis  
356 for the GDLS and GDLD pairs (which evoke a “DIFFERENT” response). This too revealed  
357 a negative correlation ( $r = -0.46$ ,  $p < 0.00005$  across all GDLS and GDLD pairs,  $r = -0.38$ ,  
358  $p < 0.0005$  for GDLS pairs; Figure 5C;  $r = -0.54$ ,  $p < 0.0005$  for GDLD pairs). We conclude  
359 that image pairs containing distinctive images elicit faster responses.

360 If distinctiveness measured from GSLS pairs is so effective in predicting responses  
361 to all other pairs, we wondered whether it can also explain the incongruence effect. To do  
362 so, we compared the net distinctiveness of congruent pairs with that of the incongruent  
363 pairs. Indeed, congruent pairs were more distinctive (average distinctiveness, mean  $\pm$  sd:

364  $3.31 \pm 0.11 \text{ s}^{-1}$  for congruent pairs,  $3.17 \pm 0.14 \text{ s}^{-1}$  for incongruent pairs,  $p < 0.005$ ,  
365 sign-rank test across 21 image pairs; Figure 5D).

366



367  
368 **Figure 5. Understanding the contribution of distinctiveness**

369 (A) Global distinctiveness ( $1/RT$ ) of each hierarchical stimulus, estimated from GSLS  
370 pairs in the global block.  
371 (B) Observed response times for GSLD pairs in the global block plotted against the  
372 net global distinctiveness estimated from panel A.  
373 (C) Observed response times for GDLS and GDLD pairs plotted against net global  
374 distinctiveness estimated from panel A.  
375 (D) Net global distinctiveness calculated for congruent and incongruent image pairs.  
376 Error bars represents standard deviation across pairs.  
377 (E) Local distinctiveness ( $1/RT$ ) for each hierarchical stimulus estimated from GSLS  
378 pairs in the local block.  
379 (F) Observed response times for GDLS pairs in the local block plotted against the net  
380 local distinctiveness estimated as in panel D.  
381 (G) Observed response times for GSLD & GDLD pairs in the local block plotted  
382 against the net local distinctiveness estimated as in panel D.  
383 (H) Net local distinctiveness calculated for congruent and incongruent image pairs.  
384 Error bar represents standard deviation across pairs.

385

386

387 **Effect of distinctiveness on same-different responses in the local block**

388 We observed similar trends in the local block. Again, we estimated distinctiveness  
389 for each image as the reciprocal of the response time to the GSLS trials in the local block  
390 (Figure 5E). It can be seen that shapes containing a local circle were more distinctive  
391 compared to shapes containing a local diamond (Figure 5E). Interestingly, the  
392 distinctiveness estimated in the local block was uncorrelated with the distinctiveness  
393 estimated in the global block ( $r = 0.16, p = 0.25$ ).

394 As with the global block, we obtained a significant negative correlation between  
395 the response times for GDLS pairs (which evoked a “SAME” response) and the net  
396 distinctiveness ( $r = -0.58, p < 0.00005$ ; Figure 5F). Likewise, we obtained a significant  
397 negative correlation between the response times of GSLD and GDLD pairs (both of which  
398 evoke “DIFFERENT” responses in the local block) with net distinctiveness ( $r = -0.22, p <$   
399  $0.0005$  across 294 GSLD and GDLD pairs; Figure 5G;  $r = -0.24, p < 0.005$  for GSLD pairs;  
400  $r = -0.18, p < 0.05$  for GDLD pairs). We conclude that distinctive images elicit faster  
401 responses.

402 Finally, we asked whether differences in net distinctiveness can explain the  
403 difference between congruent and incongruent pairs. As expected, local distinctiveness  
404 was significantly larger for congruent compared to incongruent pairs (average  
405 distinctiveness, mean  $\pm$  sd:  $3.08 \pm 0.05 \text{ s}^{-1}$  for congruent pairs,  $2.91 \pm 0.11 \text{ s}^{-1}$  for  
406 incongruent pairs,  $p < 0.00005$ , sign-rank test across 21 image pairs; Figure 5H).

407 The above analyses show that distinctiveness directly estimated from response  
408 times to identical images can predict responses to other image pairs containing non-  
409 identical images. By contrast, there is no direct subset of image pairs that can be used to  
410 measure the contribution of image dissimilarity to response times. We therefore devised  
411 a quantitative model for the response times to estimate the underlying image

412 dissimilarities and elucidate the contribution of dissimilarity and distinctiveness. Because  
413 high dissimilarity can increase response times for “SAME” responses and decrease  
414 response times for “DIFFERENT” responses, we devised two separate models for these  
415 two types of responses, as detailed below.

416

417 **Can “SAME” responses be predicted using distinctiveness and dissimilarity?**

418 Recall that “SAME” responses in the global block are made to image pairs in which  
419 the global shape is the same and local shape is different. Let AB denote a hierarchical  
420 stimulus made of shape A at the global level and B at the local level. We can denote any  
421 image pair eliciting a “SAME” response in global block as AB and AC, since the global  
422 shape will be identical. Then according to our model, the response time (SRT) taken to  
423 respond to an image pair AB & AC is given by:

424 
$$SRT(AB, AC) = k_G * GD + k_L * LD + L_{BC}$$

425 where GD is the sum of the global distinctiveness of AB and AC (estimated from  
426 GSLS pairs in the global block), LD is the sum of local distinctiveness of AB and AC  
427 (estimated from GSLS pairs in the local block),  $k_G$ ,  $k_L$  are constants that specify the  
428 contribution of GD and LD towards the response time, and  $L_{BC}$  denotes the dissimilarity  
429 between local shapes B and C. Since there are 7 possible local shapes there are only  ${}^7C_2$   
430 = 21 possible local shape terms. When this equation is written down for each GSLS pair,  
431 we get a system of linear equations of the form  $\mathbf{y} = \mathbf{Xb}$  where  $\mathbf{y}$  is a 147 x 1 vector  
432 containing the GSLS response times,  $\mathbf{X}$  is a 147 x 23 matrix containing the net global  
433 distinctiveness and net local distinctiveness as the first two columns, and 0/1 in the other  
434 columns corresponding to whether a given local shape pair is present in that image pair  
435 or not, and  $\mathbf{b}$  is a 23 x 1 vector of unknowns containing the weights  $k_G$ ,  $k_L$  and the 21

436 estimated local dissimilarities. Because there are 147 equations and only 22 unknowns,  
437 we can estimate the unknown vector **b** using linear regression.

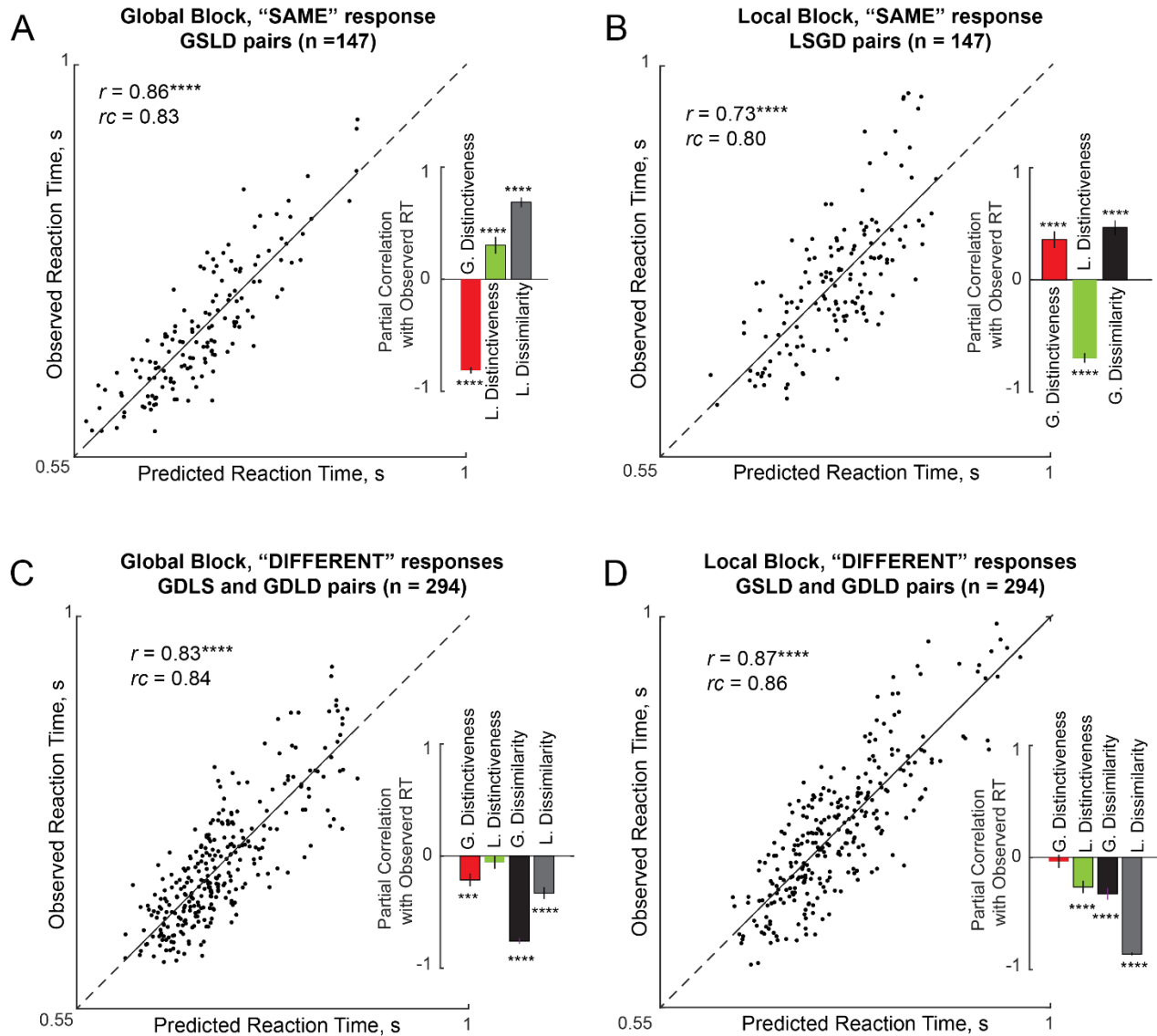
438 The performance of this model is summarized in Figure 6. The model-predicted  
439 response times were strongly correlated with the observed response times for the GSLD  
440 pairs in the global block ( $r = 0.86$ ,  $p < 0.00005$ ; Figure 6A). These model fits were close  
441 to the reliability of the data ( $rc = 0.84 \pm 0.02$ ; see Methods), suggesting that the model  
442 explained nearly all the explainable variance in the data. However the model fits do not  
443 elucidate which factor contributes more towards response times. To do so, we performed  
444 a partial correlation analysis in which we calculated the correlation between observed  
445 response times and each factor after regressing out the contributions of the other two  
446 factors. For example, to estimate the contribution of global distinctiveness, we calculated  
447 the correlation between observed response times and global distinctiveness after  
448 regressing out the contribution of local distinctiveness and the estimated local dissimilarity  
449 values corresponding to each image pair. This revealed a significant negative correlation  
450 ( $r = -0.81$ ,  $p < 0.00005$ ; Figure 6A, inset). Likewise, we obtained a significant positive  
451 partial correlation between local dissimilarities and observed response times after  
452 regressing out the other factors ( $r = 0.69$ ,  $p < 0.00005$ ; Figure 6A, inset). However, local  
453 distinctiveness showed positive partial correlation ( $r = 0.30$ ,  $p = 0.0005$ ) suggesting that  
454 locally distinctive shapes slow down responses in the global block. Thus, response times  
455 are faster for more globally distinctive image pairs, and slower for more dissimilar image  
456 pairs.

457 We obtained similar results for local “SAME” responses. As before, the response  
458 time for “SAME” responses in the local block to an image pair (AB, CB) was written as

459 
$$SRT(AB, CB) = k_G * GD + k_L * LD + G_{AC}$$

460 where SRT is the response time, GD and LD are the net global and net local  
461 distinctiveness of the images AB and CB respectively,  $k_g$ ,  $k_L$  are unknown constants that  
462 specify the contribution of the net global and local distinctiveness and  $G_{AC}$  is the  
463 dissimilarity between the global shapes A and C. As before this model is applicable to all  
464 the LSGD pairs ( $n = 147$ ), has 23 free parameters and can be solved using straightforward  
465 linear regression.

466 The model fits for local “SAME” responses is depicted in Figure 6B. We obtained  
467 a striking correlation between predicted and observed response times ( $r = 0.72$ ,  $p <$   
468  $0.00005$ ; Figure 6B). This correlation was close to the reliability of the data itself ( $rc = 0.80$   
469  $\pm 0.03$ ), suggesting that the model explains nearly all the explainable variance in the  
470 response times. To estimate the unique contribution of distinctiveness and dissimilarity,  
471 we performed a partial correlation analysis as before. We obtained a significant partial  
472 negative correlation between observed response times and local distinctiveness after  
473 regressing out global distinctiveness and global dissimilarity ( $r = -0.70$ ,  $p < 0.00005$ ;  
474 Figure 6B, inset). We also obtained a significant positive partial correlation between  
475 observed response times and global dissimilarity after factoring out both distinctiveness  
476 terms ( $r = 0.47$ ,  $p < 0.00005$ ; Figure 6B, inset). Finally, as before, global distinctiveness  
477 showed a positive correlation with local “SAME” responses after accounting for the other  
478 factors ( $r = 0.36$ ,  $p < 0.00005$ ; Figure 6B inset).



479  
480  
481  
482  
483  
484  
485  
486  
487

**Figure 6. Quantitative model for the Same-Different task**

- (A) Observed vs predicted response times for "SAME" responses in the global block. *Inset:* partial correlation between observed response times and each factor while regressing out all other factors. Error bars represents 68% confidence intervals, corresponding to  $\pm 1$  standard deviation from the mean.
- (B) Same as (A) but for "SAME" responses in the local block.
- (C) Same as (A) but for "DIFFERENT" responses in the global block.
- (D) Same as (A) but for "DIFFERENT" responses in the local block.

488 **Can “DIFFERENT” responses be predicted using distinctiveness and dissimilarity?**

489 We used a similar approach to predict “DIFFERENT” responses in the global and  
490 local blocks. Specifically, for any image pair AB and CD, the response time according to  
491 the model is written as

492 
$$DRT(AB, CD) = k_G * GD + k_L * LD - G_{AC} - L_{BD}$$

493 where DRT is the response time for making a “DIFFERENT” response, GD and  
494 LD are the net global and net local distinctiveness of the images AB and CD respectively,  
495  $k_G$ ,  $k_L$  are unknown constants that specify their contributions,  $G_{AC}$  is the dissimilarity  
496 between the global shapes A and C, and  $L_{BD}$  is the dissimilarity between the local shapes  
497 B and D. Note that, unlike the “SAME” response model, the sign of  $G_{AC}$  and  $L_{BD}$  is negative  
498 because large global or local dissimilarity should speed up “DIFFERENT” responses. The  
499 resulting model, which applies to both GDLS and GDLD pairs, consists of 44 free  
500 parameters which are the two constants specifying the contribution of the global and local  
501 distinctiveness and 21 terms each for the pairwise dissimilarities at the global and local  
502 levels respectively. As before, this is a linear model whose free parameters can be  
503 estimated using straightforward linear regression.

504 The model fits for “DIFFERENT” responses in the global block are summarized in  
505 Figure 6C. We obtained a striking correlation between observed response times and  
506 predicted response times ( $r = 0.82$ ,  $p < 0.00005$ ; Figure 6C). This correlation was close  
507 to the data reliability itself ( $rc = 0.84 \pm 0.02$ ), implying that the model explained nearly all  
508 the explainable variance in the data. To estimate the unique contributions of each term,  
509 we performed a partial correlation analysis as before. We obtained a significant negative  
510 partial correlation between observed response times and global distinctiveness after  
511 regressing out all other factors ( $r = -0.21$ ,  $p < 0.0005$ ; Figure 6C, inset). We also obtained  
512 a significant negative partial correlation between observed response times and both

513 dissimilarity terms ( $r = -0.76$ ,  $p < 0.00005$  for global terms;  $r = -0.33$ ,  $p < 0.00005$  for local  
514 terms; Figure 6C, inset). However we note that the contribution of global terms is larger  
515 than the contribution of local terms. As before, local distinctiveness did not contribute  
516 significantly to “DIFFERENT” responses in the global block ( $r = -0.06$ ,  $p = 0.34$ ; Figure  
517 6C, inset). We conclude that “DIFFERENT” responses in the global block are faster for  
518 globally distinctive image pairs, and for dissimilar image pairs.

519 We obtained similar results for “DIFFERENT” responses in the local block for  
520 GSLD and GDLD pairs. Model predictions were strongly correlated with observed  
521 response times ( $r = 0.87$ ,  $p < 0.00005$ ; Figure 6D). This correlation was close to the data  
522 reliability ( $rc = 0.85 \pm 0.01$ ) suggesting that the model explained nearly all the variance in  
523 the response times. A partial correlation analysis revealed a significant negative partial  
524 correlation for all terms except global distinctiveness (correlation between observed RT  
525 and each factor after accounting for all others:  $r = -0.26$ ,  $p < 0.00005$  for local  
526 distinctiveness,  $r = -0.04$ ,  $p = 0.55$  for global distinctiveness,  $r = -0.32$ ,  $p < 0.00005$  for  
527 global terms,  $r = -0.86$ ,  $p < 0.00005$  for local terms). In contrast to the global block, the  
528 contribution of global terms was smaller than that of the local terms. We conclude that  
529 “DIFFERENT” responses in the local block are faster for locally distinctive image pairs  
530 and for dissimilar image pairs.

531

532 **Relation between “SAME” and “DIFFERENT” model parameters**

533 Next we asked whether the dissimilarity terms estimated from “SAME” and  
534 “DIFFERENT” responses were related. In the global block, we obtained a significant  
535 positive correlation between the local dissimilarity terms (Table 1). Likewise, the global  
536 and local terms estimated from “DIFFERENT” responses were significantly correlated  
537 (Table 1). In general, only 3 out of 15 (20%) of all possible pairs were negatively

538 correlated, and the median pairwise correlation across all model term pairs was  
539 significantly above zero (median correlation: 0.14,  $p < 0.01$ ). Taken together these  
540 positive correlations imply that the dissimilarities driving the “SAME” and “DIFFERENT”  
541 responses at both global and local levels are driven by a common underlying shape  
542 representation.

543

	<b>GDS</b>	<b>GDG</b>	<b>GDL</b>	<b>LSG</b>	<b>LDG</b>	<b>LDL</b>
<b>Global SAME model, L terms</b>	1	0.54*	0.17	0.14	0.09	0.48*
<b>Global DIFFERENT model, Global terms</b>		1	0.24	0.34	0.30	0.47*
<b>Global DIFFERENT model, Local terms</b>			1	0.03	-0.08	0.14
<b>Local SAME model, Global terms</b>				1	0.11	-0.04
<b>Local DIFFERENT model, Global terms</b>					1	-0.31
<b>Local DIFFERENT model, Local terms</b>						1

544 **Table 1: Correlation between estimated dissimilarity terms within and across**  
545 **models.** Each entry represents the correlation coefficient between pairs of model terms.  
546 Asterisks represent statistical significance (\* is  $p < 0.05$ ). Column labels are identical to  
547 row labels but are abbreviated for ease of display.

548

549

## EXPERIMENT 2: VISUAL SEARCH

550        There are two main findings from Experiment 1. First, subjects show a robust  
551        global advantage and an incongruence effect in the same-different task. These effects  
552        could arise from the underlying categorization process or the underlying visual  
553        representation. To distinguish between these possibilities would require a task devoid of  
554        categorical judgments. To this end, we devised a visual search task in which subjects  
555        have to locate an oddball target among multiple identical distractors, rather than making  
556        a categorical shape judgment. Second, responses in the same-different task were  
557        explained using two factors: distinctiveness and dissimilarity, but it is not clear how these  
558        factors relate to the visual search representation.

559        We sought to address four fundamental questions. First, are the global advantage  
560        and incongruence effects present in visual search? Second, can performance in the  
561        same-different task be explained in terms of the responses in the visual search task?  
562        Third, can we understand how global and local features combine in visual search? Finally,  
563        can the dissimilarity and distinctiveness terms in the same-different model of Experiment  
564        1 be related to some aspect of the visual representations observed during visual search?

565

## METHODS

566        *Subjects.* Eight right-handed subjects (6 male, aged 23-30 years) participated in the  
567        study. We selected this number of subjects here and in subsequent experiments based  
568        on the fact that similar sample sizes have yielded extremely consistent visual search data  
569        in our previous studies (Mohan and Arun, 2012; Vighneshvel and Arun, 2013; Pramod  
570        and Arun, 2016).

571

573 *Stimuli.* We used the same set of 49 stimuli as in Experiment 1, which were created by  
574 combining 7 possible shapes at the global level with 7 possible shapes at the local level  
575 in all possible combinations.

576

577 *Procedure.* Subjects were seated approximately 60 cm from a computer. Each subject  
578 performed a baseline motor block, a practice block and then the main visual search block.  
579 In the baseline block, on each trial a white circle appeared on either side of the screen  
580 and subjects had to indicate the side on which the circle appeared. We included this block  
581 so that subjects would become familiar with the key press associated with each side of  
582 the screen, and in order to estimate a baseline motor response time for each subject. In  
583 the practice block, subjects performed 20 correct trials of visual search involving unrelated  
584 objects to become familiarized with the main task.

585 Each trial of main experiment started with a red fixation cross presented at the  
586 centre of the screen for 500 ms. This was followed by a 4 x 4 search array measuring 24°  
587 square with a spacing of 2.25° between the centers of adjacent items. Images were were  
588 slightly larger in size (1.2x) compared to Experiment 1 to ensure that the local elements  
589 were clearly visible. The search array consisted of 15 identical distractors and one oddball  
590 target placed at a randomly chosen location in the grid. Subjects were asked to locate the  
591 oddball target and respond with a key press ("Z" for left, "M" for right) within 10 seconds,  
592 failing which the trial was aborted and repeated later. A red vertical line was presented at  
593 the centre of the screen to facilitate left/right judgments.

594 Search displays corresponding to each possible image pair were presented two  
595 times, with either image in a pair as target (with target position on the left in one case and  
596 on the right in the other). Thus, there were  $49C_2 = 1,176$  unique searches and 2,352 total  
597 trials. Trials in which the subject made an error or did not respond within 10 s were

598 repeated randomly later. In practice, these repeated trials were very few in number,  
599 because subjects accuracy was extremely high (mean and std accuracy: 98.4%  $\pm$  0.7%  
600 across subjects).

601

602 *Model fitting*

603 We measured the perceived dissimilarity between every pair of images by taking  
604 the reciprocal of the average search time for that pair across subjects and trials. We  
605 constructed a quantitative model for this perceived dissimilarity following the part  
606 summation model developed in our previous study (Pramod and Arun, 2016). Let each  
607 hierarchical stimulus be denoted as AB where A is the shape at the global level and B is  
608 the local shape. The net dissimilarity between two hierarchical stimuli AB & CD is given  
609 by:

610 
$$d(AB,CD) = G_{AC} + L_{BD} + X_{AD} + X_{BC} + W_{AB} + W_{CD} + \text{constant}$$

611 where  $G_{AC}$  is the dissimilarity between the global shapes,  $L_{BD}$  is the dissimilarity between  
612 the local shapes,  $X_{AD}$  &  $X_{BC}$  are the across-object dissimilarities between the global shape  
613 of one stimulus and the local shape of the other, and  $W_{AB}$  &  $W_{CD}$  are the dissimilarities  
614 between global and local shape within each object. Thus there are 4 sets of unknown  
615 parameters in the model, corresponding to global terms, local term, across-object terms  
616 and within-object terms. Each set contains pairwise dissimilarities between the 7 shapes  
617 used to create the stimuli. Note that model terms repeat across image pairs: for instance,  
618 the term  $G_{AC}$  is present for every image pair in which A is a global shape of one and C is  
619 the global shape of the other. Writing this equation for each of the 1,176 image pairs  
620 results in a total of 1176 equations corresponding to each image pair, but with only 21  
621 shape pairs  $\times$  4 types (global, local, across, within)  $+ 1 = 85$  free parameters. The  
622 advantage of this model is that it allows each set of model terms to behave independently,

623 thereby allowing potentially different shape representations to emerge for each type  
624 through the course of model fitting.

625 This simultaneous set of equations can be written as  $\mathbf{y} = \mathbf{X}\mathbf{b}$  where  $\mathbf{y}$  is a 1,176 x  
626 1 vector of observed pairwise dissimilarities between hierarchical stimuli,  $\mathbf{X}$  is a 1,176 x  
627 85 matrix containing 0, 1 or 2 (indicating how many times a part pair of a given type  
628 occurred in that image pair) and  $\mathbf{b}$  is a 85 x 1 vector of unknown part-part dissimilarities  
629 of each type (corresponding, across and within). We solved this equation using standard  
630 linear regression (*regress* function, MATLAB).

631 The results described in the main text, for ease of exposition, are based on fitting  
632 the model to all pairwise dissimilarities, which could result in overfitting. To assess this  
633 possibility, we fitted the model each time on 80% of the data and calculated its predictions  
634 on the held-out 20%. This too yielded a strong positive correlation across many 80-20  
635 splits ( $r = 0.85 \pm 0.01$ ,  $p < 0.00005$  in all cases), indicating that the model is not overfitting  
636 to the data.

637

638

## RESULTS

639 Subjects performed searches corresponding to all possible pairs of hierarchical  
640 stimuli ( ${}^{49}C_2 = 1176$  pairs). Subjects were highly accurate in the task (mean  $\pm$  sd  
641 accuracy: 98.4%  $\pm$  0.7% across subjects).

642 Note that each image pair in visual search has a one-to-one correspondence with  
643 an image pair used in the same-different task. Thus, we have GDLS, GSLS and GDLD  
644 pairs in the visual search task. However, there are no GSLS pairs in visual search since  
645 these pairs correspond to identical images, and can have no oddball search.

646

### 647 **Is there a global advantage effect in visual search?**

648 We set out to investigate whether there is a global advantage effect in visual  
649 search. We compared searches with target differing only in global shape (i.e. GDLS pairs)  
650 with equivalent searches in which the target differed only in local shape (i.e. GSLS pairs).  
651 Two example searches are depicted in Figure 7A-B. It can be readily seen that finding a  
652 target differing in global shape (Figure 7A) is much easier than finding the same shape  
653 difference in local shape (Figure 7B).

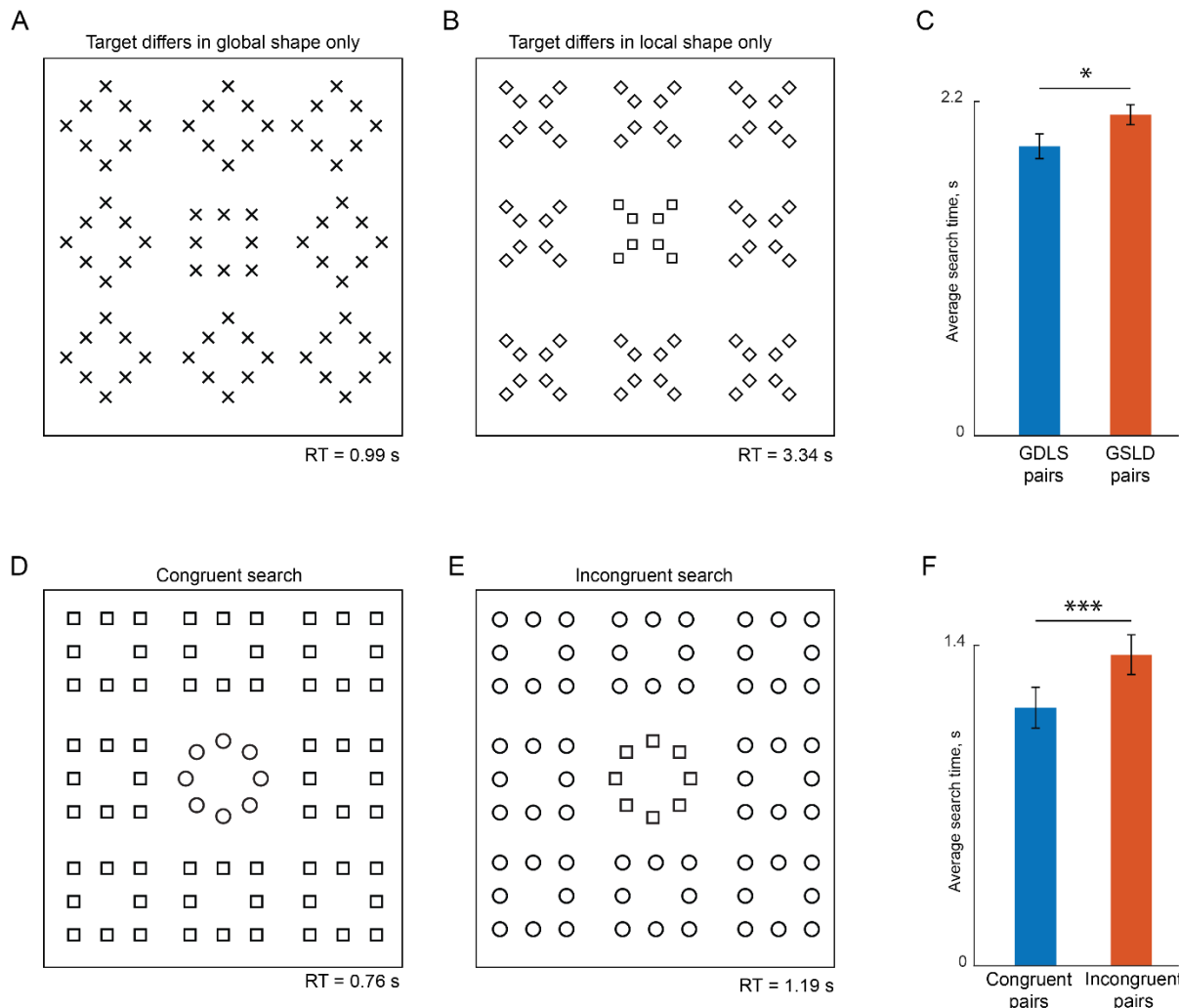
654 The above observation held true across all GDLS/GSLS searches. Subjects were  
655 equally accurate on GDLS searches and GSLS searches (accuracy, mean  $\pm$  sd: 98%  $\pm$   
656 1% for GDLS, 98%  $\pm$  1% for GSLS,  $p = 0.48$ , sign-rank test across subject-wise  
657 accuracy). However they were faster on GDLS searches compared to GSLS searches  
658 (search times, mean  $\pm$  sd:  $1.90 \pm 0.40$  s across 147 GDLS pairs,  $2.11 \pm 0.56$  s across 147  
659 GSLS pairs; Figure 7C).

660 To assess the statistical significance of this difference, we performed an ANOVA  
661 on the search times with subject (8 levels), pairs ( $7 \times 21 = 147$  levels), and hierarchical  
662 level (same-global/same-local) as factors. This revealed a significant main effect of

663 hierarchical level ( $p < 0.00005$ ). We also observed significant main effects of subject and  
664 pairs ( $p < 0.005$ ). All two-way interactions except subject x shape were also significant ( $p$   
665  $< 0.00005$ ) but these did not alter the general direction of the effect as evidenced by the  
666 fact that searches for the same global shape were harder than for the same local shape  
667 on average in 82 of 147 pairs (56%) across all subjects. We conclude that searching for  
668 a target differing in global shape is easier than searching for a target differing in local  
669 shape. Thus, there is a robust global advantage effect in visual search.

670

671



672

### Figure 7. Odd ball visual search task.

673 (A) Example search array with an oddball target differing only in global shape from the  
674 distractors. The actual experiment used 4x4 search arrays with stimuli shown as white  
675 against a black background.

676 (B) Example search array with an oddball target differing only in local shape from the  
677 distractors.

678 (C) Average response times for GDLS and GSLD pairs. Error bars represent s.e.m across  
679 subjects. Asterisks indicate statistical significance calculated using a rank-sum test  
680 across 147 pairs (\* is  $p < 0.05$ ).

681 (D) Example search array with two congruent stimuli.

682 (E) Example search array with two incongruent stimuli.

683 (F) Average response time for congruent and incongruent stimulus pairs. Error bars  
684 represent s.e.m across subjects. Asterisks indicate statistical significance using an  
685 ANOVA on response times (\*\* is  $p < 0.0005$ ).

687

688

689

690 **Is there an incongruence effect in visual search?**

691 Next we compared whether searches involving a pair of congruent stimuli were  
692 easier than those with incongruent stimuli. Two example searches are shown in Figure  
693 7D-E. It can be readily seen that search involving the congruent stimuli (Figure 7D) is  
694 easier than the search involving incongruent stimuli (Figure 7E), even though both  
695 searches involve a difference in global shape (circle to square) and a difference in local  
696 shape (circle to square).

697 To establish whether this was true across all 21 searches of this type, we  
698 performed an ANOVA on the search times with subject (8 levels), shape pair ( ${}^7C2 = 21$   
699 levels) and congruence (2 levels) as factors. This revealed a significant main effect of  
700 congruence (average search times: 1.13 s for congruent pairs, 1.36 s for incongruent  
701 pairs;  $p < 0.00005$ ). We also observed a significant main effect of subject and shape pair  
702 ( $p < 0.00005$ ), and importantly no significant interaction effects ( $p > 0.2$  for all interactions).  
703 We conclude that search involving congruent stimuli are easier than searches involving  
704 incongruent stimuli. Thus, there is a robust incongruence effect in visual search.

705

706 **Are there systematic variations in responses in the visual search task?**

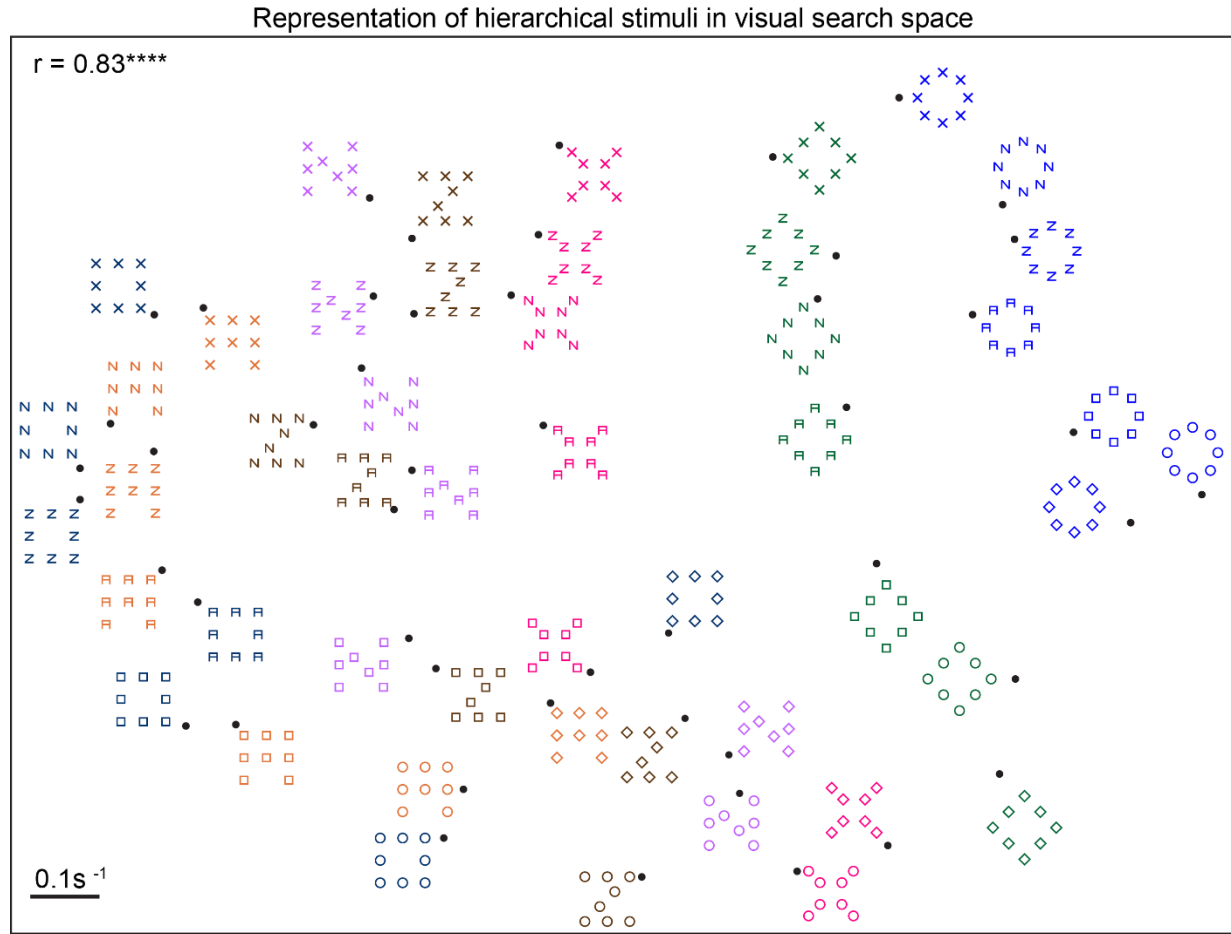
707 Having established that subjects showed a robust global advantage effect and  
708 incongruence effects, we wondered whether there were other systematic variations in  
709 their responses as well. Indeed, response times were highly systematic as evidenced by  
710 a strong correlation between two halves of the subjects (split-half correlation between RT  
711 of odd- and even-numbered subjects:  $r = 0.83$ ,  $p < 0.00005$ ).

712 Previous studies have shown that the reciprocal of search time can be taken as a  
713 measure of dissimilarity between the target and distractors. We therefore took the  
714 reciprocal of the average search time across all subjects (and trials) for each image pair

715 as a measure of dissimilarity between the two stimuli. Because we performed all pairwise  
716 searches between the hierarchical stimuli, it becomes possible to visualize these stimuli  
717 in visual search space using multidimensional scaling (MDS). Briefly, multidimensional  
718 scaling estimates the 2D coordinates of each stimulus such that distances between these  
719 coordinates match best with the observed distances. In two dimensions with 49  
720 hierarchical stimuli, there are only  $49 \times 2 = 98$  unknown coordinates that have to match  
721 the  ${}^{49}C_2 = 1,176$  observed distances. We emphasize that multidimensional scaling only  
722 offers a way to visualize the representation of the hierarchical stimuli at a glance; we did  
723 not use the estimated 2D coordinates for any subsequent analysis but rather used the  
724 directly observed distances themselves.

725 The multidimensional scaling plot obtained from the observed visual search data  
726 is shown in Figure 8. Two interesting patterns can be seen. First, stimuli with the same  
727 global shape clustered together, indicating that these are hard searches. Second,  
728 congruent stimuli (i.e. with the same shape at the global and local levels) were further  
729 apart compared to incongruent stimuli (with different shapes at the two levels), indicating  
730 that searches involving congruent stimuli are easier than incongruent stimuli. These  
731 observations concur with the global advantage and incongruence effect described above  
732 in visual search.

733



734  
735  
736  
737  
738  
739  
740  
741  
742  
743  
744

**Figure 8. Visualization of hierarchical stimuli in visual search space.**

Representation of hierarchical stimuli in visual search space, as obtained using multidimensional scaling. Stimuli of the same color correspond to the same global shape for ease of visualization. The actual stimuli were white shapes on a black background in the actual experiment. In this plot, nearby points represent hard searches. The correlation coefficient at the top right indicates the degree of match between the two-dimensional distances depicted here with the observed search dissimilarities in the experiment. Asterisks indicate statistical significance: \*\*\* is  $p < 0.00005$ .

745

746 **How do global and local shape combine in visual search?**

747 So far we have shown that the global advantage and incongruence effects in the  
748 same-different task also arise in the visual search task, suggesting that these effects are  
749 intrinsic to the underlying representation of these hierarchical stimuli. However, these  
750 findings do not provide any fundamental insight into the underlying representation or how  
751 it is organized. For instance, why are incongruent shapes more similar than congruent  
752 shapes? How do global and local shape combine?

753 To address these issues, we asked whether search for pairs of hierarchical stimuli  
754 can be explained in terms of shape differences and interactions at the global and local  
755 levels. To build a quantitative model, we drew upon our previous studies in which the  
756 dissimilarity between objects differing in multiple features was found to be accurately  
757 explained as a linear sum of part-part dissimilarities (Pramod and Arun, 2014, 2016;  
758 Sunder and Arun, 2016). Consider a hierarchical stimulus AB, where A represents the  
759 global shape and B is the local shape. Then, according to the model (which we dub the  
760 multiscale part sum model), the dissimilarity between two hierarchical stimuli AB & CD  
761 can be written as a sum of all possible pairwise dissimilarities between the parts A, B, C  
762 and D as follows (Figure 6A):

$$763 \quad d(AB,CD) = G_{AC} + L_{BD} + X_{AD} + X_{BC} + W_{AB} + W_{CD} + \text{constant}$$

764 where  $G_{AC}$  is the dissimilarity between the global shapes,  $L_{BD}$  is the dissimilarity  
765 between the local shapes,  $X_{AD}$  &  $X_{BC}$  are the across-object dissimilarities between the  
766 global shape of one stimulus and the local shape of the other, and  $W_{AB}$  &  $W_{CD}$  are the  
767 dissimilarities between global and local shape within each object. Since there are 7  
768 possible global shapes, there are  ${}^7C_2 = 21$  pairwise global-global dissimilarities  
769 corresponding to  $G_{AB}$ ,  $G_{AC}$ ,  $G_{AD}$ , etc, and likewise for L, X and W terms. Thus in all the  
770 model has 21 part-part relations x 4 types + 1 constant = 85 free parameters. Importantly,

771 the multiscale part sum model allows for completely independent shape representations  
772 at the global level, local level and even for comparisons across objects and within object.  
773 The model works because the same global part dissimilarity  $G_{AC}$  can occur in many  
774 shapes where the same pair of global shapes A & C are paired with various other local  
775 shapes.

776

### 777 **Performance of the part sum model**

778 To summarize, we used a multiscale part sum model that explains the dissimilarity  
779 between two hierarchical stimuli as a sum of pairwise shape comparisons across multiple  
780 scales. To evaluate model performance, we plotted the observed dissimilarities between  
781 hierarchical stimuli against the dissimilarities predicted by the part sum model (Figure 9B).  
782 This revealed a striking correlation ( $r = 0.88$ ,  $p < 0.00005$ ; Figure 9B). This high degree  
783 of fit matches the reliability of the data (mean  $\pm$  sd reliability:  $rc = 0.84 \pm 0.01$ ; see  
784 Methods).

785 This model also yielded several insights into the underlying representation. First,  
786 because each group of parameters in the part sum model represent pairwise part  
787 dissimilarities, we asked whether they all reflect a common underlying shape  
788 representation. To this end we plotted the estimated part relations at the local level (L  
789 terms), the across-object global-local relations (X terms) and the within-object relations  
790 (W terms) against the global part relations (G terms). This revealed a significant  
791 correlation for all terms (correlation with global terms:  $r = 0.60$ ,  $p < 0.005$  for L terms,  $r =$   
792  $0.75$ ,  $p < 0.00005$  for X terms,  $r = -0.60$ ,  $p < 0.005$  for W terms; Figure 9C). This is  
793 consistent with the finding that hierarchical stimuli and large/small stimuli are driven by a  
794 common representation at the neural level (Sripati and Olson, 2009).

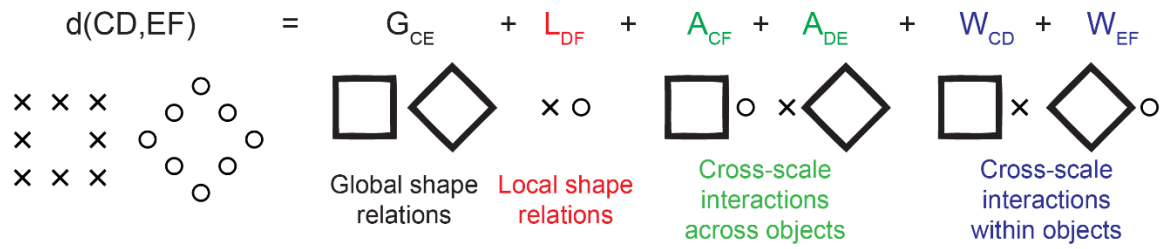
795           Second, cross-scale within-object (W terms) were negative (average: -0.04, p <  
796 0.005, sign-rank test on 21 within-object terms). In other words, the effect of within-object  
797 dissimilarity is to increase overall dissimilarity when global and local shapes are similar  
798 to each other and decrease overall dissimilarity when they are dissimilar.

799           Third, we visualized this common shape representation using multidimensional  
800 scaling on the pairwise global coefficients estimated by the model. The resulting plot  
801 (Figure 9D) reveals a systematic arrangement whereby similar global shapes are nearby.  
802 Ultimately, the multiscale part sum model uses this underlying part representation  
803 determines the overall dissimilarity between hierarchical stimuli.

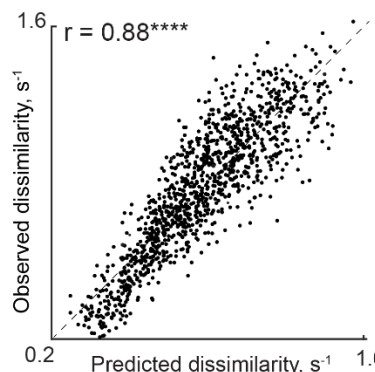
804

805

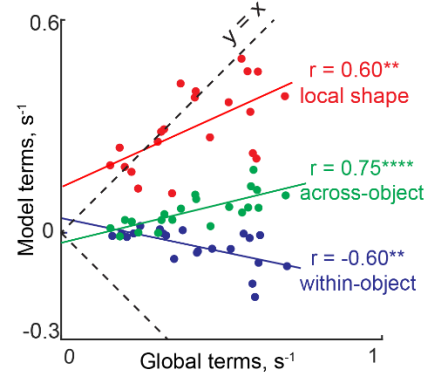
A



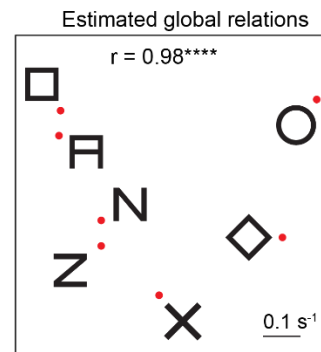
B



C



D



806  
807

### Figure 9. Global and local shape integration in hierarchical stimuli

808 (A) We investigated how global and local shape combine in visual search using the  
809 multiscale part sum model. According to the model, the dissimilarity between two  
810 hierarchical stimuli can be explained as a weighted sum of shape differences at the  
811 global level, local level and cross-scale differences across and within objects (see  
812 text).

813 (B) Observed dissimilarity plotted against predicted dissimilarity for all 1,176 object pairs  
814 in the experiment.

815 (C) Local and cross-scale model terms plotted against global terms. Coloured lines  
816 indicates the corresponding best fitting line. Asterisks indicate statistical significance:  
817 \*\*\* is  $p < 0.0005$ , \*\*\*\* is  $p < 0.00005$ .

818 (D) Visualization of global shape relations recovered by the multiscale model, as obtained  
819 using multidimensional scaling analysis.

820

821

822 **Can the multiscale model explain the global advantage and incongruence effect?**

823 Having established that the full multiscale part sum model yielded excellent  
824 quantitative fits, we asked whether it can explain the global advantage and incongruence  
825 effects.

826 First, the global advantage effect in visual search is the finding that shapes differing  
827 in global shape are more dissimilar than shapes differing in local shape. This is explained  
828 by the multiscale part sum model by the fact that global part relations are significantly  
829 larger in magnitude compared to local terms (average magnitude across 21 pairwise  
830 terms:  $0.42 \pm 0.17 \text{ s}^{-1}$  for global,  $0.30 \pm 0.11 \text{ s}^{-1}$  for local,  $p < 0.005$ , sign-rank test).

831 Second, how does the multiscale part sum model explain the incongruence effect?  
832 We first confirmed that the model shows the same pattern as the observed data (Figure  
833 10A). To this end we examined how each model term in the model works for congruent  
834 and incongruent shapes (Figure 10B). First, note that the terms corresponding to global  
835 and local shape relations are identical for both congruent and incongruent stimuli so these  
836 cannot explain the incongruence effect. However, congruent and incongruent stimuli differ  
837 in the cross-scale interactions both across and within stimuli. For a congruent pair, which  
838 have the same shape at the global and local level, the contribution of within-object terms  
839 is zero, and the contribution of across-object terms is non-zero, resulting in an overall  
840 larger dissimilarity (Figure 10B). In contrast, for an incongruent pair, the within-object  
841 terms are negative and across-object terms are zero, leading to a smaller overall  
842 dissimilarity.

843 To summarize, the multiscale model explains qualitative features of visual search  
844 such as the global advantage and incongruence effects, and explains visual search for  
845 hierarchical stimuli using a linear sum of multiscale part differences. The excellent fits of  
846 the model indicate that shape information combines linearly across multiple scales.

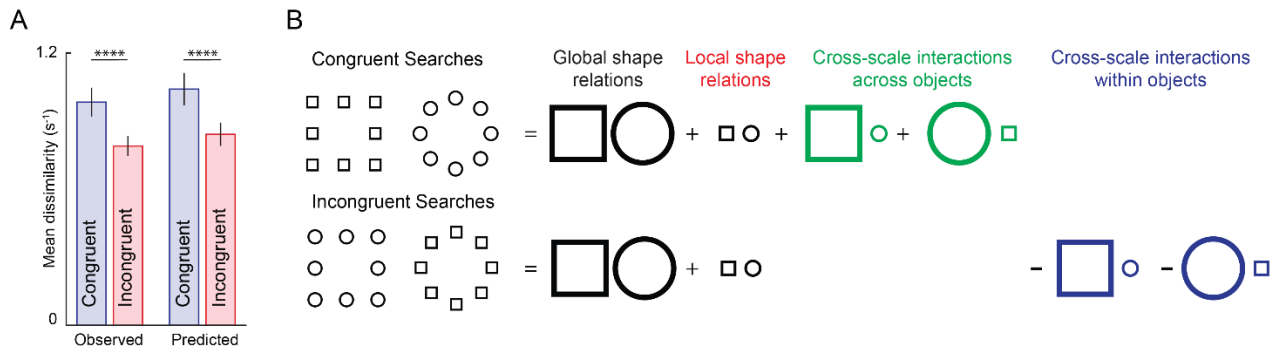


**Figure 10. Incongruence effect in visual search.**

(A) Average dissimilarity for congruent and incongruent image pairs for observed dissimilarities (*left*) and dissimilarities predicted by the multiscale part sum model (*right*). Error bars indicate sd across image pairs. Asterisks indicate statistical significance, as calculated using an ANOVA, with conventions as before.

(B) Schematic illustrating how the multiscale model predicts the incongruence effect. For both congruent and incongruent searches, the contribution of global and local terms in the model is identical. However for congruent searches, the net dissimilarity is large because cross-scale across terms are non-zero and within-object terms are zero (since the same shape is present at both scales). In contrast, for incongruent searches, the net dissimilarity is small because across-object terms are zero (since the local shape of one is the global shape of the other) and within-object terms are non-zero and negative.

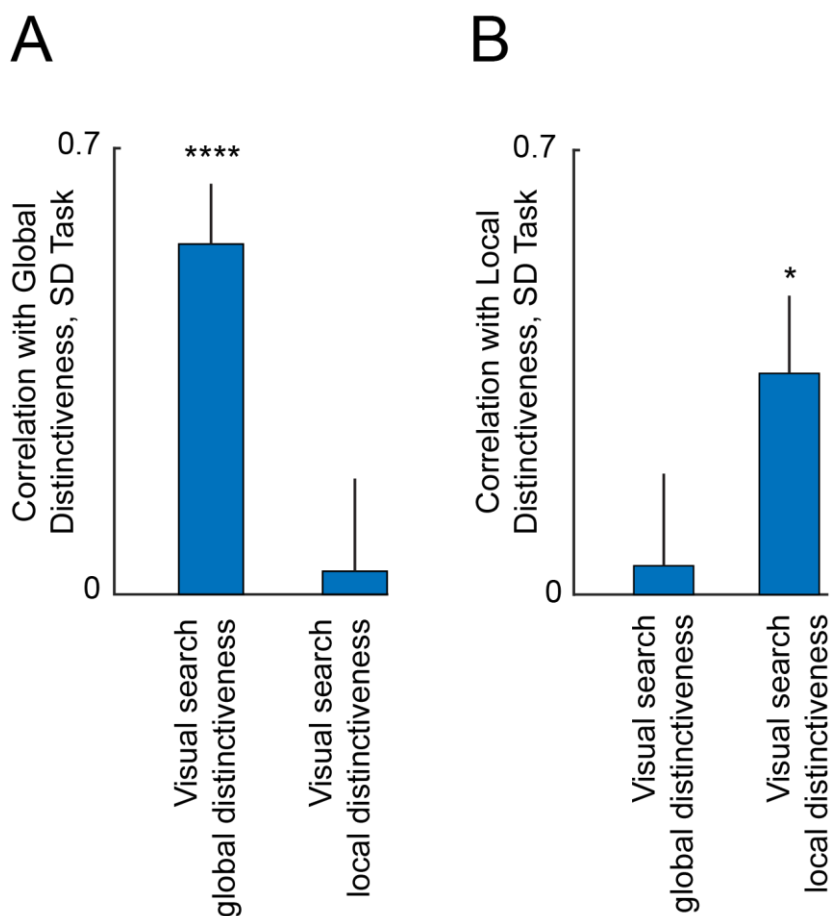
## Relating same-different model parameters to visual search

Recall that the responses in the same-different task were explained using two

864 factors, distinctiveness and dissimilarity (Figure 6). We wondered whether these factors  
865 are related to any aspect of the visual search representation.

We first asked whether the distinctiveness of each image as estimated from the GSLS pairs in the same-different task is related to the hierarchical stimulus representation in visual search. We accordingly calculated a measure of global distinctiveness in visual search as follows: for each image, we calculated its average dissimilarity ( $1/RT$  in visual search) to all other images with the same global shape. Likewise, we calculated local search distinctiveness as the average dissimilarity between a given image and all other images with the same local shape. We then asked how the global and local distinctiveness estimated from the same-different task are related to the global and local search distinctiveness estimated from visual search.

875 We obtained a striking double-dissociation: global distinctiveness estimated in the  
876 same-different task was correlated only with global but not local search distinctiveness ( $r$   
877  $= 0.55$ ,  $p < 0.00005$  for global search distinctiveness;  $r = 0.036$ ,  $p = 0.55$  for local search  
878 distinctiveness; Figure 11A). Likewise, local distinctiveness estimated in the same-  
879 different task was correlated only with local search distinctiveness but not global  
880 distinctiveness ( $r = 0.35$ ,  $p < 0.05$  for local search distinctiveness;  $r = 0.05$ ,  $p = 0.76$  for  
881 global search distinctiveness; Figure 11B).



882  
883 **Figure 11. Relation between same-different model parameters and visual search**  
884 (A) Correlation between distinctiveness estimated from GSLS trials in the global block  
885 of the same-different (SD) task with global and local search distinctiveness. Error  
886 bars represents 68% confidence intervals, corresponding to  $\pm 1$  standard deviation  
887 from the mean.  
888 (B) Correlation between distinctiveness estimated from GSLS trials in the local block  
889 of the same-different task with global and local search distinctiveness.

890

891 Next we investigated whether the global and local shape dissimilarity terms  
892 estimated from the same-different task were related to the global and local terms in the  
893 part-sum model. Many of these correlations were positive and significant (Table 2),  
894 suggesting that all dissimilarities are driven by a common shape representation.

895 We conclude that both distinctiveness and dissimilarity terms in the same-different  
896 task are systematically related to the underlying representation in visual search.

897

Same-Different Model Terms	Correlation with Visual Search Global Terms	Correlation with Visual Search Local Terms
<b>Same-Different Task, Global Block</b>		
Same model Local Terms	0.47*	0.76****
Different model Global Terms	0.69****	0.82****
Different Model Local Terms	0.02	0
<b>Same-Different task, Local Block</b>		
Same model Local Terms	0.37	0.11
Different model Global Terms	0.38	0.21
Different Model Local terms	0.14	0.6**

898 **Table 2. Comparison of model parameters across tasks.** Each entry represents the  
899 correlation coefficient between model terms estimated from the same-different task and  
900 global and local terms from the visual search model. Asterisks represent statistical  
901 significance (\* is  $p < 0.05$ , \*\*\*\* is  $p < 0.00005$  etc).

902

### 903 Comparison of part-sum model with other models

904 The above results show that search for hierarchical stimuli is best explained using  
905 the reciprocal of search time (1/RT), or search dissimilarity. That models based on 1/RT  
906 provides a better account than RT-based models was based on our previous findings  
907 (Vighneshvel and Arun, 2013; Pramod and Arun, 2014, 2016; Sunder and Arun, 2016).

908 To reconfirm this finding, we fit RT and 1/RT based models to the data in this experiment.  
909 Indeed, 1/RT based models provided a better fit to the data (Section S1).

910 The above results are also based on a model in which the net dissimilarity is based  
911 on part differences at the global and local levels as well as cross-scale differences across  
912 and within object. This raises the question of whether simpler models based on a subset

913 of these terms would provide an equivalent fit. However, this was not the case: the full  
914 model yielded the best fits despite having more free parameters (Section S1).

915

## 916 **Simplifying hierarchical stimuli**

917 One fundamental issue with hierarchical stimuli is that the global shape is formed  
918 using the local shapes, making them inextricably linked. We therefore wondered whether  
919 hierarchical stimuli can be systematically related to simpler stimuli in which the global and  
920 local shape are independent of each other. We devised a set of “interior-exterior” shapes  
921 whose representation in visual search can be systematically linked to that of the  
922 hierarchical stimuli, and thereby simplifying their underlying representation. Even here,  
923 we found that the dissimilarity between interior-exterior stimuli can be explained as a  
924 linear sum of shape relations across multiple scales (Section S2). Moreover, changing  
925 the position, size and grouping status of the local elements leads to systematic changes  
926 in the model parameters (Section S3-5). These findings provide a deeper understanding  
927 of how shape information combines across multiple scales.

928

## GENERAL DISCUSSION

929       Classic perceptual phenomena such as the global advantage and incongruence  
930    effects have been difficult to understand because they have been observed during shape  
931    detection tasks, where a complex category judgment is made on a complex feature  
932    representation. Here, we have shown that these phenomena are not a consequence of  
933    the categorization process but rather are explained by intrinsic properties of the  
934    underlying shape representation. Moreover, this underlying representation is governed  
935    by a simple rule whereby global and local features combine linearly.

936       Our findings in support of this conclusion are: (1) Global advantage and  
937    incongruence effects are present in a same-different task as well as in a visual search  
938    task devoid of any shape categorization; (2) Responses in the same-different task were  
939    accurately predicted using two factors: dissimilarity and distinctiveness; (3) Dissimilarities  
940    in visual search were explained using a simple linear rule whereby the net dissimilarity is  
941    a sum of pairwise multiscale shape dissimilarities. Below we discuss how these results  
942    relate to the existing literature.

943

### 944   **Explaining global advantage and incongruence effects**

945       We have shown that the global advantage and incongruence effects also occur in  
946    visual search, implying that they are intrinsic properties of the underlying representation.  
947    Moreover we show that this representation is organized according to a simple linear rule  
948    whereby global and local features combine linearly (Figure 9). This model provides a  
949    simple explanation of both effects. The global advantage occurs simply because global  
950    part relations are more salient than local relations (Figure 9C). The interference effect  
951    occurs because congruent stimuli are more dissimilar (or equivalently, more distinctive)

952 than incongruent stimuli, which in turn is because the within-object part differences are  
953 zero for part relations (Figure 10).

954 Finally, it has long been observed that the global advantage and interference  
955 effects vary considerably on the visual angle, eccentricity and shapes of the local  
956 elements (Navon, 1977; Navon and Norman, 1983; Kimchi, 1992; Poirel et al., 2008). Our  
957 results offer a systematic approach to understand these variations: the multiscale model  
958 parameters varied systematically with the position, size and grouping status of the local  
959 elements (Section S3-5).

960

## 961 **Understanding same-different task performance**

962 We have found that image-by-image variations in response times in the same-  
963 different task can be accurately explained using a quantitative model. To the best of our  
964 knowledge, there are no such quantitative models for the same-different task. According  
965 to our model, responses in the same-different task are driven by two factors: dissimilarity  
966 and distinctiveness.

967 The first factor is the dissimilarity between two images in a pair. Notably, it has  
968 opposite effects on “SAME” and “DIFFERENT” responses. This makes intuitive sense  
969 because if images are more dissimilar, it should make “SAME” responses harder and  
970 “DIFFERENT” responses easier. It is also consistent with the common models of  
971 decision-making (Gold and Shadlen, 2002) and categorization (Ashby and Maddox, 1994;  
972 Mohan and Arun, 2012), where responses are triggered when a decision variable  
973 exceeds a criterion value. In this case, the decision variable is the dissimilarity.

974 The second factor is distinctiveness. Response times were faster for images that  
975 are more distinctive, i.e. far away from other stimuli. This makes intuitive sense because  
976 nearby stimuli can act as distractors and slow down responses. Importantly, the

977 distinctiveness of an image in the global block matched best with its average distance  
978 from all other stimuli with the same global shape (Figure 11A). Conversely the  
979 distinctiveness in the local block matched best with its average distance from all other  
980 shapes with the same local shape (Figure 11B). This finding is concordant with norm-  
981 based accounts of object representations (Sigala et al., 2002; Leopold et al., 2006),  
982 wherein objects are represented relative to an underlying average. We speculate that this  
983 underlying average is biased by the level of attention, making stimuli distinctive at the  
984 local or global level depending on the block. Testing these intriguing possibilities will  
985 require recording neural responses during global and local processing.

986

### 987 **Linearity in visual search**

988 We have found that the net dissimilarity between hierarchical stimuli can be  
989 understood as a linear sum of shape relations across multiple scales. This finding is  
990 consistent with our previous studies showing that the net dissimilarity in visual search is  
991 a linear sum of elemental feature differences (Pramod and Arun, 2014) as well as of local  
992 and configural differences (Pramod and Arun, 2016). Likewise, the net dissimilarity in a  
993 search for a target among multiple distractors can be understood as a sum of the  
994 dissimilarity of the constituent searches (Vighneshvel and Arun, 2013). More recently, we  
995 have demonstrated that knowledge of a forthcoming target adds linearly to bottom-up  
996 dissimilarity (Sunder and Arun, 2016). Taken together, these findings suggest that a  
997 variety of factors combine in visual search according to a simple linear rule.

998

## REFERENCES

999

1000 Arun SP (2012) Turning visual search time on its head. *Vision Res* 74:86–92.

1001 Ashby FG, Maddox WT (1994) A response time theory of separability and integrality in

1002 speeded classification. *J Math Psychol* 38:423–466.

1003 Avarguès-Weber A, Dyer AG, Ferrah N, Giurfa M (2015) The forest or the trees:

1004 preference for global over local image processing is reversed by prior experience in

1005 honeybees. *Proceedings Biol Sci* 282:20142384.

1006 Behrmann M, Avidan G, Leonard GL, Kimchi R, Luna B, Humphreys K, Minshew N (2006)

1007 Configural processing in autism and its relationship to face processing.

1008 *Neuropsychologia* 44:110–129.

1009 Bahrle AM, Bellugi U, Delis D, Marks S (1989) Seeing either the forest or the trees:

1010 dissociation in visuospatial processing. *Brain Cogn* 11:37–49.

1011 Brainard DH (1997) The Psychophysics Toolbox. *Spat Vis* 10:433–436.

1012 Cavoto KK, Cook RG (2001) Cognitive precedence for local information in hierarchical

1013 stimulus processing by pigeons. *J Exp Psychol Anim Behav Process* 27:3–16.

1014 Fink GR, Halligan PW, Marshall JC, Frith CD, Frackowiak RS, Dolan RJ (1996) Where in

1015 the brain does visual attention select the forest and the trees? *Nature* 382:626–628.

1016 Franceschini S, Bertoni S, Gianesini T, Gori S, Facoetti A (2017) A different vision of

1017 dyslexia: Local precedence on global perception. *Sci Rep* 7:17462.

1018 Freedman DJ, Miller EK (2008) Neural mechanisms of visual categorization: Insights from

1019 neurophysiology. *Neurosci Biobehav Rev* 32:311–329.

1020 Gerlach C, Poirel N (2018) Navon's classical paradigm concerning local and global

1021 processing relates systematically to visual object classification performance. *Sci Rep*

1022 8:324.

1023 Gerlach C, Starrfelt R (2018) Global precedence effects account for individual differences

1024 in both face and object recognition performance. *Psychon Bull Rev* 25:1365–1372.

1025 Gold JI, Shadlen MN (2002) Banburismus and the brain: Decoding the relationship

1026 between sensory stimuli, decisions, and reward. *Neuron* 36:299–308.

1027 Han S, Jiang Y, Gu H (2004) Neural substrates differentiating global/local processing of

1028 bilateral visual inputs. *Hum Brain Mapp* 22:321–328.

1029 Han S, Weaver JA, Murray SO, Kang X, Yund EW, Woods DL (2002) Hemispheric

1030 asymmetry in global/local processing: effects of stimulus position and spatial

1031 frequency. *Neuroimage* 17:1290–1299.

1032 Kimchi R (1992) Primacy of wholistic processing and global/local paradigm: a critical

1033 review. *Psychol Bull* 112:24–38.

1034 Kimchi R (1994) The role of wholistic/configural properties versus global properties in

1035 visual form perception. *Perception* 23:489–504.

1036 Lachmann T, Van Leeuwen C (2008) Different letter-processing strategies in diagnostic

1037 subgroups of developmental dyslexia. *Cogn Neuropsychol* 25:730–744.

1038 Lamb MR, Robertson LC (1990) The effect of visual angle on global and local reaction

1039 times depends on the set of visual angles presented. *Percept Psychophys* 47:489–

1040 496.

1041 Leopold D a, Bondar I V, Giese M a (2006) Norm-based face encoding by single neurons

1042 in the monkey inferotemporal cortex. *Nature* 442:572–575.

1043 Liu L, Luo H (2019) Behavioral oscillation in global/local processing: Global alpha

1044 oscillations mediate global precedence effect. *J Vis* 19:12.

1045 Malinowski P, Hübner R, Keil A, Gruber T (2002) The influence of response competition

1046 on cerebral asymmetries for processing hierarchical stimuli revealed by ERP

1047 recordings. *Exp brain Res* 144:136–139.

1048 Miller J, Navon D (2002) Global precedence and response activation: evidence from

1049 LRP<sub>s</sub>. *Q J Exp Psychol A* 55:289–310.

1050 Mohan K, Arun SP (2012) Similarity relations in visual search predict rapid visual  
1051 categorization. *J Vis* 12:19–19.

1052 Morrison DJ, Schyns PG (2001) Usage of spatial scales for the categorization of faces,  
1053 objects, and scenes. *Psychon Bull Rev* 8:454–469.

1054 Navon D (1977) Forest before trees: The precedence of global features in visual  
1055 perception. *Cogn Psychol* 9:353–383.

1056 Navon D, Norman J (1983) Does global precedence really depend on visual angle? *J Exp  
1057 Psychol Hum Percept Perform* 9:955–965.

1058 Oliva A, Schyns PG (1997) Coarse blobs or fine edges? Evidence that information  
1059 diagnosticity changes the perception of complex visual stimuli. *Cogn Psychol* 34:72–  
1060 107.

1061 Pitteri E, Mongillo P, Carnier P, Marinelli L (2014) Hierarchical stimulus processing by  
1062 dogs (*Canis familiaris*). *Anim Cogn* 17:869–877.

1063 Poirel N, Pineau A, Mellet E (2008) What does the nature of the stimuli tell us about the  
1064 Global Precedence Effect? *Acta Psychol (Amst)* 127:1–11.

1065 Pramod RT, Arun SP (2014) Features in visual search combine linearly. *J Vis* 14:1–20.

1066 Pramod RT, Arun SP (2016) Object attributes combine additively in visual search. *J Vis*  
1067 16:8.

1068 Robertson LC, Lamb MR (1991) Neuropsychological contributions to theories of  
1069 part/whole organization. *Cogn Psychol* 23:299–330.

1070 Romei V, Driver J, Schyns PG, Thut G (2011) Rhythmic TMS over Parietal Cortex Links  
1071 Distinct Brain Frequencies to Global versus Local Visual Processing. *Curr Biol*  
1072 21:334–337.

1073 Sigala N, Gabbiani F, Logothetis NK (2002) Visual categorization and object  
1074 representation in monkeys and humans. *J Cogn Neurosci* 14:187–198.

1075 Slavin MJ, Mattingley JB, Bradshaw JL, Storey E (2002) Local-global processing in  
1076 Alzheimer's disease: an examination of interference, inhibition and priming.  
1077 *Neuropsychologia* 40:1173–1186.

1078 Song Y, Hakoda Y (2015) Lack of global precedence and global-to-local interference  
1079 without local processing deficit: A robust finding in children with attention-  
1080 deficit/hyperactivity disorder under different visual angles of the Navon task.  
1081 *Neuropsychology* 29:888–894.

1082 Sripati AP, Olson CR (2009) Representing the forest before the trees: a global advantage  
1083 effect in monkey inferotemporal cortex. *J Neurosci* 29:7788–7796.

1084 Sunder S, Arun SP (2016) Look before you seek: Preview adds a fixed benefit to all  
1085 searches. *J Vis* 16:3.

1086 Tanaka H, Fujita I (2000) Global and local processing of visual patterns in macaque  
1087 monkeys. *Neuroreport* 11:2881–2884.

1088 Ullman S, Vidal-Naquet M, Sali E (2002) Visual features of intermediate complexity and  
1089 their use in classification. *Nat Neurosci* 5:682–687.

1090 Vighneshvel T, Arun SP (2013) Does linear separability really matter? Complex visual  
1091 search is explained by simple search. *J Vis* 13:1–24.

1092

## 1093 ACKNOWLEDGEMENTS

1094 SPA was supported by Intermediate and Senior Fellowships from the Wellcome-  
1095 DBT India Alliance (Grant #: 500027/Z/09/Z and IA/S/17/1/503081).

1096

1097

1098

1099 **AUTHOR CONTRIBUTIONS**

1100 GJ & SPA designed experiments, GJ collected data, GJ & SPA analysed and  
1101 interpreted data and wrote the manuscript.

1102